1 **The genomic landscape, causes, and consequences of extensive phylogenomic discordance**
2 **in murine rodents**

3

4 Gregg W. C. Thomas[1,2,*], Jonathan J. Hughes[3,4], Tomohiro Kumon[5], Jacob S. Berv[3,6], C. Erik
5 Nordgren[5], Michael Lampson[5], Mia Levine[5], Jeremy B. Searle[3], Jeffrey M. Good[1]

6

7 [1]*Division of Biological Sciences, University of Montana, Missoula, MT, 59801.*

8 [2]*Informatics Group, Harvard University, Cambridge, MA, 02138*

9 [3]*Department of Ecology and Evolutionary Biology, Cornell University, Ithaca, NY, 14853.*

10 [4]*Department of Evolution, Ecology, and Organismal Biology, University of California Riverside,*
11 *Riverside, CA, 92521*

12 [5]*Department of Biology, University of Pennsylvania, Philadelphia, PA, 19104*

13 [6]*Department of Ecology and Evolutionary Biology, University of Michigan, Ann Arbor, MI,*
14 *48109*

15

16 [*]Corresponding author

17 E-mail: gthomas@fas.harvard.edu

18

19 **Abstract**

20 A species tree is a central concept in evolutionary biology whereby a single branching phylogeny
21 reflects relationships among species. However, the phylogenies of different genomic regions often
22 differ from the species tree. Although tree discordance is widespread in phylogenomic studies, we
23 still lack a clear understanding of how variation in phylogenetic patterns is shaped by genome
24 biology or the extent to which discordance may compromise comparative studies. We
25 characterized patterns of phylogenomic discordance across the murine rodents – a large and
26 ecologically diverse group that gave rise to the laboratory mouse and rat model systems.
27 Combining recently published linked-read genome assemblies for seven murine species with other
28 available rodent genomes, we first used ultra-conserved elements (UCEs) to infer a robust time-
29 calibrated species tree. We then used whole genomes to examine finer-scale patterns of
30 discordance across ~12 million years of divergence. We found that proximate chromosomal
31 regions tended to have more similar phylogenetic histories. There was no clear relationship
32 between local tree similarity and recombination rates in house mice, but we did observe a
33 correlation between recombination rates and average similarity to the species tree. We also
34 detected a strong influence of linked selection whereby purifying selection at UCEs led to
35 appreciably less discordance. Finally, we show that assuming a single species tree can result in
36 substantial deviation from the results with gene trees when testing for positive selection under
37 different models. Collectively, our results highlight the complex relationship between
38 phylogenetic inference and genome biology and underscore how failure to account for this
39 complexity can mislead comparative genomic studies.

40

41 **Keywords:** *phylogenetic discordance, murine rodents, molecular evolution recombination,*
42 *genomics, mouse*

43 **Significance Statement**

44 Genomic data has demonstrated that when sequences from multiple species are compared,
45 different regions of the genome exhibit different phylogenetic histories. These discordant histories
46 could be due to either biological processes, such as ancestral variation or introgression, or artifacts
47 of the inference process. We use the genomes of several murine rodents to distinguish how features
48 of the genome, such as recombination rates, genes, and other conserved regions, affect this
49 discordance across the genome. Considering the prevalence of discordance across the genome, we
50 also test how using a single species tree, a common practice, affects inferences from tests for
51 positive selection. Our study shows that conserved genomic loci exhibit lower amounts of
52 discordance, and that discordance can negatively affect inferences of selection.

Introduction

Phylogenies are the unifying concept in understanding the evolution of species, traits, and genes. However, extensive high-throughput sequencing data has now revealed that evolutionary relationships between species are often not be well represented by a single phylogeny (Edwards 2009; Hahn and Nakhleh 2016). While a dominant signal of bifurcating speciation usually exists (*i.e.*, a species tree), phylogenetic signal that may disagree with species relationships can arise from ancestral polymorphisms (incomplete lineage sorting; ILS), gene flow (introgression), and gene duplication and loss (Maddison 1997). The theoretical prediction of phylogenetic discordance has long been appreciated (Hudson 1983; Pamilo and Nei 1988; Maddison 1997; Rosenberg 2002), but empirical evidence now emphasizes just how extensive discordance can be among a set of species (Feng, et al. 2022; Gable, et al. 2022; Smith, et al. 2023). For example, studies of birds (Jarvis, et al. 2014), mammals (Ferreira, et al. 2021; Lopes, et al. 2021; Foley, et al. 2024), plants (Pease, et al. 2016), and insects (Sun, et al. 2021; He, et al. 2023) have found that with extensive taxon sampling and genomic data, highly supported species tree topologies are rarely or never exactly recovered in the underlying gene trees. Whereas these examples highlight the prevalence of phylogenetic discordance across the tree of life, we still lack a clear understanding of how phylogenetic patterns are shaped by the details of genome biology or the extent to which discordance may compromise inferences from comparative studies that assume a singular species history.

In practice, failure to acknowledge and account for phylogenetic discordance could severely affect biological inference. Analyses of molecular evolution are usually performed on a gene-by-gene basis (Pond, et al. 2005; Yang 2007; Hu, et al. 2019; Kowalczyk, et al. 2019), but it is still common practice to assume a single genome-wide species tree for each locus. For gene-based analyses, using the wrong tree may cause erroneous inferences of positive directional selection, convergent evolution, and genome-wide inferences of correlated rate variation (Mendes, et al. 2016). Phylogenetic discordance can also affect how continuous traits are reconstructed across phylogenies, as the genes that underly these traits may not follow the species history (Avise and Robinson 2008; Hahn and Nakhleh 2016; Mendes, et al. 2018; Hibbins, et al. 2023). In these instances, phylogenetic discordance may need to be characterized and incorporated into the experimental and analytical design. Alternatively, if a researcher's primary questions are focused on reconstructing the evolutionary history of speciation (*i.e.*, the species tree), then phylogenetic discordance may obscure the true signal of speciation (Fontaine, et al. 2015; Foley, et al. 2024). In this case, knowledge about patterns of discordance across genomes could inform decisions about locus selection, data filtering, and model parameters during species tree reconstruction.

Given these considerations, a better understanding of the genomic context of phylogenetic discordance is warranted. Although often conceptualized primarily as a stochastic consequence of population history (Maddison 1997), patterns of phylogenetic discordance are likely to be non-random and dependent on localized patterns of genetic drift, natural selection, recombination, and mutation (Johri, et al. 2022). Discordance due to ILS ultimately depends on effective population sizes across the branches of the phylogeny (Pamilo and Nei 1988; Degnan and Rosenberg 2006)

93   and, therefore, should covary with any process that influences local patterns of genetic diversity
94   (*e.g.*, linked negative or positive selection). Likewise, discordance due to introgression may be
95   influenced by selection against incompatible alleles or positive selection for beneficial variants
96   (Lewontin and Birch 1966; Jones, et al. 2018). Selection, ILS, and introgression, are expected to
97   leave different genomic signals that should allow us to test hypotheses about both the cause and
98   the scale of phylogenetic discordance (Huson, et al. 2005; Kulathinal, et al. 2009; Green, et al.
99   2010; Vanderpool, et al. 2020). Yet the genomic context of phylogenetic discordance has remained
100   elusive. For example, localized patterns of phylogenetic discordance should be influenced by
101   patterns of recombination (Hudson and Kaplan 1988) and simulation studies confirm that the
102   closer two regions are in the genome, the more history they share (Slatkin and Pollack 2006;
103   McKenzie and Eaton 2020). However, empirical studies have been inconclusive regarding the
104   relationship between discordance and recombination rates, ranging from no relationship in great
105   apes (Hobolth, et al. 2007), a weak positive correlation in house mice (White, et al. 2009), a strong
106   positive correlation broadly across primates (Rivas-Gonzalez, et al. (2023), or increased
107   discordance in regions of lower recombination (Scally, et al. 2012; Pease and Hahn 2013). Thus,
108   it remains unclear how phylogenetic discordance scales locally across the genome as a function of
109   recombination and the strength of linked selection, pointing to the need for empirical studies in
110   systems with sufficient genomic resources to explore the causes of discordance.
111   To investigate the causes and consequences of phylogenetic discordance, we took
112   advantage of genomic resources available for house mice (*Mus musculus*). This rodent species is
113   one of the most important mammalian model systems for biological and biomedical research and
114   is embedded within a massive radiation of rats and mice (Murinae). This ecologically diverse and
115   species-rich group is comprised of over 600 species and makes up >10% of all mammalian species,
116   and yet is only about 15 million years old, making this system an excellent choice for phylogenetic
117   studies over both short and long timescales. Despite the power of evolution-guided functional and
118   biomedical analysis (Christmas, et al. 2023), relatively few murine genomes have been sequenced
119   outside of *Mus* and *Rattus*.
120   We analyze recently sequenced genomes for seven murine species (*Mastomys natalensis*,
121   *Hylomyscus alleni*, *Praomys delectorum*, *Rhabdomys dilectus*, *Grammoyms dolichurus*, *Otomoys*
122   *typus*, and *Rhynchomys soricoides*) sampled from across this radiation (Kumon, et al. 2021). We
123   combine these new genomes with previously sequenced genomes and genomic resources from the
124   *M. musculus* model system to study phylogenetic relationships within Murinae as well as the
125   landscape of discordance along rodent chromosomes. We first inferred a species tree for these and
126   other sequenced rodent genomes, focusing on signals derived from commonly used ultra-
127   conserved elements (UCEs). We used these UCE data to infer a robust, time-calibrated phylogeny
128   of sequenced murine rodents, providing a useful resource for future comparative studies within
129   this important group. Using this species tree, we then used a subset of whole genomes to study
130   how phylogenetic discordance is related to species-level inferences of relatedness, recombination
131   rate, and patterns of molecular evolution. Using genetic maps and functional annotation from the
132   powerful house mouse system, we test several hypotheses linking spatial patterns of discordance

133 to genetic drift, natural selection, and recombination. Finally, we show how the use of a single
134 species-tree impacts gene-level inferences from common molecular evolution tests for natural
135 selection in these species. Collectively, our results advance our understanding of how core features
136 of genome biology influence underlying phylogenetic patterns, the extent to which established
137 model system resources can be leveraged for broader phylogenetic studies, and the consequences
138 of ignoring phylogenetic uncertainty.
139
140 **Results**

141 *Estimation of a murine species tree*

142 Using a concatenated dataset of 2,632 aligned ultra conserved elements (UCEs), we inferred a
143 species tree of 18 murine rodent species (Figure 1; Table S1) that recovered the same relationships
144 as previous reconstructions of Murinae using a small number of loci (Lecompte, et al. 2008;
145 Steppan and Schenk 2017). The species tree inferred from a quartet-based summary of the gene
146 tree topologies was identical to the concatenated tree (Figure S1). While bootstrap and SH-aLRT
147 values provided high support to our inferred species trees (Figure 1), we found evidence for
148 considerable discordance across individual UCE phylogenies. The five shortest branches in the
149 concatenated tree had a site concordance factor (sCF) of less than 50%, suggesting that alternate
150 resolutions of the quartet had equivocal support (Figure S2). Gene concordance factors (gCF) for
151 each branch in the species tree were on aggregate much higher, with all but four branches
152 supported by almost every gene tree in the analysis and with the lowest values likely being driven
153 by a several short internal branches (Figure S2). This pattern was recapitulated using a quartet-
154 based summary method (Figs. S1 and S3). At the two most discordant nodes (E and J in Figure 1),
155 the recovered topology was supported by approximately one third of all gene trees.
156 We estimated divergence times for the inferred concatenated phylogeny (Figure 1; Table
157 S2) using four fossil calibration points (Table S3). The murid and cricetid groups had an estimated
158 divergence time of 22.66 Ma (node A in Figure 1) followed by the Murinae and the Gerbillinae at
159 21.34 Ma (B), albeit with wide confidence intervals (CI) in both cases. The core Murinae (C) *sensu*
160 Steppan et al. (2005) are inferred to have arisen 13.11 Ma (CI: 11.42 – 15.10). Hydromyini then
161 split off at 12.15 Ma (D, CI: 11.10 – 13.51) followed by Otomyini and Arvicanthini at 11.70 Ma
162 (E, fossil calibration from Kimura, et al 2015). The remaining Murine tribes evolved in rapid
163 succession, with Apodemini diverging from Murini and Praomyini at 10.84 Ma (F). Murini and
164 Praomyini then split at 10.19 Ma (H). The two *Rattus* species in our dataset were inferred to have
165 diverged 2.01 Ma (Q, CI: 1.26 – 2.30). This dated UCE phylogeny is congruent with previous
166 works (Lecompte, et al. 2008; Steppan and Schenk 2017) and provides context on the evolutionary
167 timescale upon which we next describe the genomic landscape of phylogenetic discordance across
168 a collection of murine genomes.
169
170 *The landscape of phylogenetic discordance along murine genomes*

171 We analyzed genome-wide phylogenetic histories of six recently sequenced murine rodent
172 genomes and the *M. musculus* reference genome spanning approximately 12 million years of
173 divergence (see Figure 1). Using the *M. musculus* coordinate system, we partitioned and aligned
174 263,389 non-overlapping 10 kb windows from these seven species (Table S1). After filtering
175 windows in repetitive regions or with low phylogenetic signal, we recovered 163,765 trees with
176 an average of 616 informative sites per window (Figure S4).

177   Phylogenetic discordance was pervasive within and between chromosomes. We inferred
178 597 of the 945 possible unique rooted topologies among six species (when specifying *R. soricoides*
179 as the outgroup) across all chromosomes. The number of unique topologies per chromosome
180 ranged from 75 to 218 (mean = 141). However, just four different topologies were ranked in the
181 top three per chromosome. (Fig 2A; File S1) and only nine trees were present at a frequency above
182 1%. Among these, the top three topologies only differed in the ordering of the clade containing
183 *Hylomyscus alleni, Mastomys natalensis,* and *Praomys delectorum* (HMP clade). This clade also
184 showed the second lowest concordance in the species tree inferred from UCEs (Figure 1, node J).
185 These three topologies comprise between 13-15% of all recovered topologies (Figure 2).
186 Interestingly, the least common of these three trees (13.1%) matched the topology recovered via
187 concatenation of all coding regions and the species tree recovered from UCEs (Figure 1). That is,
188 the robustly inferred species tree did not match the evolutionary relationships inferred for over
189 85% of the genome.

190   While visual inspection revealed no clear partitioning of topological structures along
191 chromosomes (*e.g.*, Figure 2C), we found that phylogenies were not randomly distributed across
192 mouse chromosomes. Using the weighted Robinson-Foulds metric, we found that tree similarity
193 between windows decayed logarithmically along chromosomes (Figure 3A and B), and the
194 distance at which tree similarity appeared random varied considerably among chromosomes
195 ranging from 0.15 Megabases (Mb) on chromosome 17 to 141.29 Mb on the chromosome 2 (Figure
196 3C, Figure S5). While chromosomes 2, 7, 9, and 11 were autosomal outliers with distances between
197 windows to random-like trees exceeding 25 Mb, the average distance among all other autosomes
198 was only 2.1 Mb. The rates at which phylogenetic similarity decayed tended to be inversely
199 proportional to the distance at which two randomly drawn phylogenies lost similarity (Figure 3D).

200   Next, we performed a pairwise alignment of the reference mouse and rat genomes to assess
201 how large structural variations, such as inversions and translocations, may influence our inferences
202 of phylogenetic relatedness along the genome. These species span the deepest divergence of the
203 sample for which we assessed genome-wide discordance, so the level of large structural variation
204 present among them should give us an idea of the amount of ancestral variation in our sample. The
205 mouse and rat genomes were mostly co-linear for large, aligned chunks, with large translocations
206 and inversions on mouse chromosomes 5, 8, 10, 13, and 16 (Figure S6). We also observe large-
207 scale inversions on chromosome 16. We found that, while most chromosomes were co-linear
208 between mouse and rat, the average size of the 307,275 contiguously aligned chunks averages
209 under 10 kb, with the average distance between aligned segments being between 2,380 bp on the
210 mouse genome and 4,927 bp on the rat chromosome (Figure S7). This pattern presents two major

211 implications for our analyses. First, we could not transpose the coordinate system from mouse to
212 rat with enough resolution to use genetic maps from rat. Second, most other structural variations
213 in our sample appear likely to be small insertions of transposable elements (e.g., SINEs ~150-500
214 bp, LINEs ~4-7kb; Platt, et al. 2018) that should have a negligible effect on discordance analyses
215 since our window size is much larger and we excluded windows that were made up of mostly
216 repeats.
217
218 *Discordance with recombination rate and other genomic features*

219 Using markers from genetic crosses within *M. musculus* (Shifman, et al. 2006; Cox, et al. 2009)
220 we examined whether regions with high recombination also showed more phylogenetic
221 discordance over short genetic distances when compared to regions with low recombination.
222 Specifically, we calculated recombination rates within 5 Mb windows (Figure S8) and then
223 measured tree similarity between the first and last 10 kb window ($R^2 = 3.0e-9$; $p = 0.99$; Figure
224 4A) and the rate at which tree similarity changes between the first 10 kb window and every other
225 10 kb window ($R^2 = 0.003$; $p = 0.11$; Figure 4B). Surprisingly, we found no relationship between
226 tree similarity and recombination rates measured at this scale. However, we did observe a slight
227 positive correlation between recombination rate and dissimilarity to the species tree when
228 averaging wRF over all 10 kb window trees within a 5 Mb recombination window ($R^2 = 0.05$; $p = $
229 7.6e-8; Figure 4C). We also examined regions of the genome centered on recombination hotspots
230 identified in *M. musculus* (Smagulova, et al. 2011) and found that these regions had significantly
231 slower rates of decay in similarity over genomic distance compared to windows that were not
232 centered on hotspots ($p = 0.019$; Figure 5A), and that they were also significantly more
233 phylogenetically similar over short distances ($p = 0.015$; Figure 5B). Thus, when taken as a whole,
234 we found that regions of higher recombination rates in house mice did not show more local
235 phylogenetic discordance *per se* but did tend to show more discordance relative to the genome-
236 wide species tree.
237   Evolutionary relationships around certain conserved genomic features may also be shaped
238 by locally reduced effective population sizes due to a history of pervasive linked negative or
239 positive selection. To test for this, we measured tree similarity in 10 kb windows around all
240 annotated protein-coding genes, ultra-conserved elements (UCEs), and protein-coding genes
241 identified as evolving rapidly (*i.e.*, significantly elevated d_N/d_S) due to positive directional selection
242 and compared these patterns relative to chromosome-wide trends (i.e., windows without annotated
243 features). In general, UCEs showed more local phylogenetic similarity among adjacent windows
244 (i.e., less discordance) than regions surrounding recombination hotspots ($p = 2.42e-12$), coding
245 genes ($p = 4.65e-14$), rapidly evolving coding genes ($p = 1.56e-6$), and windows that did not
246 include any of these features ($p = 5.02e-14$; Figure 5A). In contrast, protein-coding genes
247 (including rapidly evolving genes) were indistinguishable from background rates of discordance
248 observed in windows without annotated genomic features (Figure 5A). Likewise, UCEs were also
249 much more similar to the overall species tree when compared to any other feature (Figure 5B).
250 Unlike our test of local discordance, protein-coding genes also showed less species tree

7

251 discordance than windows containing no features or recombination hotspots, but the effect was
252 much less pronounced than observed at UCEs.
253
254 *Consequences of tree specification on analyses of molecular evolution*

255 Next, we examined how phylogenetic discordance influenced inferences on the evolution of
256 protein-coding sequences. Among a set of 22,261 *M. musculus* protein-coding transcripts, the
257 average distance between the start and end of the coding sequence was 37.02 kb, or roughly 4 non-
258 overlapping 10 kb windows. At this distance, tree similarity is predicted to diminish considerably
259 (*e.g.*, by 0.10 wRF units), such that the phylogenetic history of individual genes may often contain
260 some phylogenetic discordance (Mendes and Hahn 2016; Mendes, et al. 2019). We also found that
261 out of the 67,566 times the coding sequence in a gene overlapped with a 10 kb window, the inferred
262 topology of the gene tree exactly matched the topology of the corresponding window tree only
263 11% of the time. Thus, the common practice of inferring gene trees on concatenated coding exons
264 from a single transcript is still likely averaging over multiple possible albeit correlated histories.
265 Finally, we tested how tree misspecification might impact standard d_N/d_S based
266 phylogenetic analyses for positive directional selection. Specifically, we used the still common
267 practice of assuming a single species tree for all genes and compared that to using individually
268 inferred gene trees in three common statistical tests for positive selection: PAML's M1a vs. M2a
269 test (Yang 2007), HyPhy's BUSTED test (Murrell, et al. 2015), and HyPhy's aBSREL test (Smith,
270 et al. 2015a). We found that many genes were inferred as having experienced positive directional
271 selection when using a single species tree, but not when using gene trees and vice versa (Figure
272 6). The extent to which the single species tree differed from the gene trees for the different types
273 of selection test is documented in Table 1. For BUSTED, we observe that 28% of genes inferred
274 as having evolved under positive directional selection when using the gene tree were not inferred
275 when using the concatenated species tree. The opposite was true for M1a vs. M2a, where, among
276 genes showing inconsistent evidence for positive selection across the two scenarios, 76% do so
277 when using the concatenated species tree but not individual gene trees. In general, genes found to
278 be evolving under positive selection using both tree types tended to be more concordant with the
279 species tree than those that had evidence for positive selection either using only the concatenated
280 tree or the gene tree (Figure 6).
281
282 **Discussion**

283 Phylogenies provide insight into the relationships of species and serve as a framework for asking
284 questions about molecular and trait evolution. However, phylogenetic histories vary extensively
285 across regions of a genome as a simple consequence of population genetic processes, and
286 evolutionary relationships between species may not often be well represented by a single
287 representative species-level phylogeny. Here, we combine the resources of the house mouse (*Mus*
288 *musculus*) with new and recently published (Kumon et al. 2021) genomes from seven species to
289 understand the systematics of murine rodents and causes and consequences of phylogenetic

290 discordance along murine genomes. These new analyses help to place this important model system
291 in a stronger evolutionary context and begin to fill the gap in genome sampling of murine rodents,
292 which, despite their exceptional morphological and ecological diversity and species richness, have
293 had relatively few whole genomes sequenced. We use these genomic resources to study the
294 landscape of phylogenetic discordance across the genome, understand how recombination and
295 natural selection shape phylogenetic histories, and evaluate how assuming a single evolutionary
296 history can compromise the study of molecular evolution in an important biomedical model
297 system.
298
299 *Phylogenomic relationships of murine rodent lineages from conserved genomic regions*

300 The extraordinary species richness of murine rodents complicates phylogenetic analyses because
301 of the resources required to sample, sequence, and analyze such widely distributed taxa. Earlier
302 work either attempted to resolve specific groups such as *Mus* (Lundrigan, et al. 2002; Suzuki, et
303 al. 2004) and *Apodemus* (Serizawa, et al. 2000; Liu, et al. 2004), or to uncover broader
304 relationships across the subfamily (Martin, et al. 2000; Steppan, et al. 2005) based on a few genetic
305 markers. Lecompte et al. (2008) provided one of the earliest well-supported phylogenetic
306 reconstructions from across Murinae and the tribal classifications they proposed remain generally
307 supported. More recent work has increased the number of taxa sampled, both for analyses of
308 Murinae specifically (Pagès, et al. 2016) and for their placement within Muridae and Muroidea
309 (Schenk, et al. 2013; Steppan and Schenk 2017; Rowe, et al. 2019) albeit based on a limited
310 number of loci. More recent studies have greatly expanded the number of loci used for
311 phylogenetic inference (Mikula, et al. 2021), including the use of 1,245 exons (Roycroft, et al.
312 2020) and 1,360 exons (Roycroft, et al. 2021), but have focused on specific tribes within Murinae.
313 Our inferred species tree based on 2,632 UCEs from 18 species across the radiation (Figure
314 1) is consistent with previous studies (Lecompte, et al. 2008; Steppan and Schenk 2017; Aghova,
315 et al. 2018). Branch support was uniformly high, and gene trees unambiguously support the tribal
316 classification of Lecompte, et al. (2008). However, four shorter branches show more substantial
317 gene tree discordance (Figure 1, branches D, E, H, and J), with two recovered clades (E and J)
318 being supported by less than half of all gene trees. We also estimated divergence times on our
319 inferred species tree using four fossil calibration points (Table S3), recovering times that are
320 roughly consistent with the relatively young estimates found by (Steppan and Schenk 2017) (see
321 Supplement). This dated species tree provides an evolutionary timescale to evaluate the genomic
322 landscape of phylogenetic discordance across ~12 my of murine evolution.
323
324 *The genomic landscape of phylogenetic discordance*

325 Limiting the number and nature of the loci used to resolve species relationships is often useful to
326 get an initial picture of the history of speciation across many taxa. However, such targeted
327 approaches may fail to capture the degree of discordance driven by incomplete lineage sorting and
328 introgression (Alexander, et al. 2017; Chan, et al. 2020; Vanderpool, et al. 2020; Alda, et al. 2021).

Our results highlight the limitations of reduced marker-based approaches and the general relationships between phylogenetic patterns and functional attributes of the genome in several interesting ways. Using the house mouse genome annotation, we found that the species tree inferred from only genes or UCEs did not match evolutionary relationships inferred for over 85% of the genome. Although similar frequencies were observed among these three most common trees (Figure 2), the topology robustly inferred from genes or UCEs was not that common overall and only the third most frequent topology among 10 kb windows genome-wide. This result was driven mainly by discordance among three more closely related (Praomyini) species sampled for this study, which had nodes with low concordance in the UCE species tree (Fig 1, node J). In the window analysis, each alternate topology of this clade occurred at a frequency of ~14% while the rest of the topology remained consistent with the species tree (Figure 2), indicating that the alternate topologies are caused by high levels of ILS at these nodes. Increased discordance at unresolved nodes is a common feature of phylogenomic datasets. These patterns illustrate how extensive discordance can arise even in a small sample of species and underscores that a single inferred species tree often may not capture the history of individual regions of the genome.

Given the fundamental role that recombination should play in shaping patterns of genetic variation within genomes, it is reasonable to assume that patterns of ILS should be broadly shaped by local recombination rate. We did not observe a clear relationship between local recombination rates in mice (*M. musculus*) and the degree of local phylogenetic discordance (i.e., phylogenetic similarity over 5 Mb intervals). However, we did find that regions of high recombination rate tended to be more discordant with the inferred species tree, in line with findings in mammals (Pease and Hahn 2013; Foley, et al. 2023; Rivas-Gonzalez, et al. 2023) and *Drosophila* (Pease and Hahn 2013). Recombination rates evolve fairly rapidly both within (Kong, et al. 2002; Cox, et al. 2009; Stapley, et al. 2017) and between mammalian species (Jensen-Seaman, et al. 2004; Ptak, et al. 2005; Stevison, et al. 2016; Stapley, et al. 2017) likely due, in part, to the high turnover of hotspots due to the changing landscape of binding sites for PRDM9 (Baudat, et al. 2010; Singhal, et al. 2015). Similar to findings in great apes (Hobolth, et al. 2007), our results suggest that high-resolution genetic maps from a single species provide some weak predictive value for understanding broader patterns of species tree discordance. However, these limited estimates may not be predictive of finer-scale patterns in a sample spanning over 12 million years of mammalian evolution (but see Foley, et al. 2023). Overall, the evolution of recombination landscapes across closely related species remains an important empirical question in evolutionary genetics (Dapper and Payseur 2017), especially as the generation of chromosome-scale genome assemblies continues to greatly outpace estimates of patterns of recombination within those genomes.

One source of evolution in the recombination map may be changes in synteny. Our reference-guided analyses assume collinearity between *Mus* and the other lineages we are comparing (*i.e.*, no karyotype variation), at least at the window-based scale we are comparing variation. Structural variation, including substantial variation in chromosome numbers, is likely to be widespread in rodents (Stanyon, et al. 1999; Yalcin, et al. 2011; Romanenko, et al. 2012; Keane, et al. 2014) and has the potential to skew our results when comparing tree similarity between

369   regions of the genome using multiple species. Generating chromosome-scale assemblies may
370   prove limiting for some non-*Mus* and *Rattus* species given that tissue resources for this group are
371   derived from natural history collections that often lack high molecular weight DNA. Nonetheless,
372   whole genome alignments between mouse and rat indicate high degrees of chromosomal synteny
373   and co-linearity (Fig S6), suggesting that many regions will be colinear in our sample.

374   Natural selection reduces the effective population size (N_e) of genomic regions through
375   genetic hitchhiking of variation linked to the fixation of positively selected mutations (i.e.,
376   selective sweeps; Maynard Smith and Haigh 1974; Kaplan, et al. 1989) and the purging of
377   deleterious mutations (i.e., background selection; Charlesworth, et al. 1993; Hudson and Kaplan
378   1995). Thus, variation in parameters dependent on N_e – such as standing levels of nucleotide
379   variation and patterns of incomplete lineage sorting – should be reduced by linkage to functional
380   elements subject to selection (Johri, et al. 2022). Consistent with this, we observed the lowest rates
381   of local discordance (Figure 5A) and overall gene tree/species tree discordance (Figure 5B) near
382   UCEs when compared to all other genomic features we studied. These results suggest that a history
383   of recurrent purifying selection on UCEs (Katzman, et al. 2007) strongly reduces patterns of
384   discordance through a persistent local reduction in N_e. In contrast, protein coding genes showed
385   rates of local discordance that were similar to background levels, even when considering genes
386   rapidly evolving due to positive directional selection (Figure 5A). However, both classes of genes
387   did show less species tree discordance than background consistent with previous results (Scally,
388   et al. 2012; Rivas-Gonzalez, et al. 2023), but this effect was much weaker than as observed at
389   UCEs (Figure 5B). Collectively, these data suggest that the frequency and strength of selection
390   plays an important role in structuring patterns of incomplete lineage sorting across the genome
391   over deeper evolutionary timescales.

392   One practical consequence of this is that phylogenetic inferences based on UCE markers
393   would seem less prone to discordance and may provide cleaner estimates of species tree history
394   than randomly chosen or protein-coding regions. Indeed, windows centered on UCEs have a higher
395   degree of similarity to the species tree than other genomic features (i.e., 17% concordance with
396   the species tree, versus 13% genome-wide or 15% for protein-coding genes). However, it is worth
397   noting that UCEs are also more likely to provide a potentially misleading underestimate of
398   genome-wide levels of discordance. Given this relationship, species tree inferences based on UCEs
399   should likely not, for example, be extended to related population genetic parameters of interest
400   (*e.g.*, ancestral population sizes, estimates population genetic diversity), and could mislead the
401   reconstruction of protein (see below) or trait evolution across phylogenies (Avise and Robinson
402   2008; Hahn and Nakhleh 2016; Mendes, et al. 2018; Hibbins, et al. 2023). Finally, despite the
403   relative ease of generating UCE data, such markers are likely unsuitable for genetic inferences
404   within populations given the pervasive effects of linked selection.

405

406   *Discordance and Molecular Evolution*

407   We also found that the choice of tree topology significantly affects the results from various
408   common tests for positive selection. Previous studies have used simulations to show that tree

misspecification can lead to incorrect placement of substitutions on branches, possibly leading to spurious results for tests of positive directional selection within empirical datasets (Mendes and Hahn 2016). Here, we use empirical data in mice to document the extent that using local gene trees versus assuming an overall species tree may shape inferences of positive directional selection on protein-coding sequences.

For each of the three selection tests run (*i.e.*, HyPhy's BUSTED and aBSREL and PAML's M1a vs. M2a) some genes showed evidence of positive selection whether the species tree or gene tree was used. In contrast, many other genes had signatures of positive selection restricted only to a single specification strategy. As expected, genes that were sensitive to specification strategy tended to more discordant with the species tree, while the genes that showed evidence of positive selection regardless of the tree used had levels of discordance comparable to all genes (85%, Figure 6, numbers in parentheses). This suggests that specifying a potentially incorrect tree (*e.g.*, the species tree when the underlying gene trees are discordant) can often affect inferences of positive selection. The magnitude and direction of these biases were dependent on the underlying model. So-called branch-site models that allow substitution rates to vary among both branches and codon sites, such as HyPhy's BUSTED and aBSREL models, resulted in more genes inferred with evidence for positive selection when using the local gene tree. This suggests that using a single species tree for branch-site tests may reduce the power to detect positive selection. On the other hand, models that only allow rates to vary among sites, such as PAML's M1a vs. M2a test, showed an increase in the number of cases where there was positive selection detected with the species trees but not with the local gene tree. As these inferences are based on empirical data, the actual phylogenetic histories are not known and both specification strategies could result in errors. That said, our findings suggest that phylogenetic discordance may bias results towards spurious increases in d_N/d_S that mimics positive directional selection in some instances, or loss of power to detect selection in other cases and that the magnitude and direction of these biases vary by model type.

These results have wide-ranging implications for phylogenetics and comparative genomic analysis. First, it is imperative that when testing a specific locus for positive selection, discordance among loci must be accounted for. This is most easily achieved by simply using the gene tree (or other locus type) as input to the test for selection (Good, et al. 2013; Mendes and Hahn 2016; Roycroft, et al. 2021). However, as Mendes and Hahn (2016) pointed out, this may not completely mask the effects of discordance on substitution rates, as sites within a single gene may still have evolved under different histories because of within-gene recombination. Indeed, we found that tree similarity diminished at scales that were less than the average genomic distance between the beginning and end of a coding sequence in mice (~37 kb in this data set). Nevertheless, we suggest that starting with an inferred gene tree is advisable whenever possible, followed by a secondary analysis of evidence for within-gene variation in phylogenetic history. Our results also imply that studies of molecular evolution may benefit from approaches that reduce genome-wide levels of discordance, such as through *post hoc* pruning of species that disproportionately contribute to unresolved nodes.

Incorporating discordance into a comparative framework is not trivial and many comparative genomic methods assume a single species tree that test for changes in substitution rates in a phylogeny (Pollard, et al. 2010; Hu, et al. 2019; Partha, et al. 2019). Even methods that allow the use of different trees for different loci (like PAML and HyPhy) are still commonly applied with a single species tree across loci (Carbone, et al. 2014; Foote, et al. 2015; van der Valk, et al. 2021; Treaster, et al. 2023). Our suggestions are on the simple assumption that the results from the local gene tree are more likely to be correct, but, as noted above, this may not always be the case given that errors can also occur during gene tree inference. Still, our results confirm that the use of a single tree for all loci for such tests that rely on accurate estimation of substitution rates are likely to lead to both inaccurate inferences of positive selection. We strongly encourage the use of individual gene trees for such analyses.

Conclusions

Murine rodents as a study system allow us to use the high-quality *M. musculus* genome to examine fine-scale patterns and effects of phylogenetic discordance along chromosomes. Our analysis reveals how discordance varies with genome biology across evolutionary timescales, as well as the limits of inference inherent to extrapolating information from a single model system to a phylogenetic sample. We also demonstrate how phylogenetic discordance can mislead common tests for selection if only a single species tree is used. Overall, our results emphasize that progress in comparative genomics requires a detailed understanding of the heterogeneous biological signals in phylogenomic datasets.

Our results help illuminate the complexities of phylogenomic datasets and the need to accommodate phylogenetic discordance in genome-wide analyses. Genomic data now dominate the study of both population genetics and phylogenetics, and these once disparate fields are increasingly unified. Species tree phylogenies are an emergent pattern of the genome-wide accumulation of stochastic and directional population-level processes that cannot be fully captured or modeled by a single history (Steenwyk, et al. 2023). Importantly, phylogenetic discordance is not limited to closely related populations or species and is expected to leave persistent signals over deep evolutionary timescales (Oliver 2013). In turn, the use of tree-based frameworks for studying evolution (at any timescale) must incorporate the population-level processes that shape phylogenetic discordance. There appear to be relatively few tree-based applications where the use of a single evolutionary history is appropriate. Indeed, failure to account for phylogenetic discordance can lead to spurious inferences of molecular evolution (Figure 6; Mendes, et al. (2016)), trait evolution (Avise and Robinson 2008; Hahn and Nakhleh 2016), and even species diversification (Louca and Pennell 2020). Similar to the need for robust baseline models in population genomic inference (Johri, et al. 2022), understanding the causes and landscape of phylogenetic discordance constitutes a critical first step in phylogenomic analysis (Mirarab, et al. 2021; Steenwyk, et al. 2023).

Materials & Methods

Sample collection and assembly

We collected genomes from 16 murine species and two other rodents from several sources, including NCBI and several recently sequenced in Kumon, et al. (2021) (see Table S1 for full list of samples and sources). We also report the genome of *Otomys typus* (FMNH 230007) from Ethiopia in 2015. While DNA extraction and sequencing on the 10x Genomics platform for *O. typus* is the same as described in (Kumon, et al. 2021), the library quality for this sample was too low for chromosome level assembly. Here, we instead assembled it into scaffolds with the express purpose of obtaining UCEs for phylogenetic analysis. Adapters and low-quality bases were trimmed from the reads using illumiprocessor (Faircloth 2013), which makes use of functions from trimmomatic (Bolger, et al. 2014). All cleaned reads were de novo assembled using ABySS 2.3.1 (Jackman, et al. 2017) with a Bloom filter (Bloom 1970) de Bruijn graph. The final *O. typus* scaffold assembly was 2.14GB (N50=9,211; L50=64,014; E-size=12,790).

In parallel, for six of these species (see Figure 1; Table S1), we generated reference-based pseudo-assemblies with iterative mapping using an updated version pseudo-it v3.1.1 (Sarver, et al. 2017) that incorporates insertion-deletion variation to minimize reference bias in our genome-wide phylogenetic analyses and to maintain collinearity between assemblies (https://github.com/goodest-goodlab/pseudo-it). We used the *Mus musculus* (mm10) genome as the reference for our pseudo-assembly approach. Briefly, pseudo-it maps reads from each sample to the reference genome with BWA (Li 2013), calls variants with GATK HaplotypeCaller (Poplin, et al. 2018), and filters SNPs and indels and generates a consensus assembly with bcftools (Danecek, et al. 2021). The process is repeated, each time using the previous iteration's consensus assembly as the new reference genome to which reads are mapped. In total, we did three iterations of mapping for each sample.

Ultraconserved element (UCE) retrieval and alignment

We first set out to reconstruct a phylogeny of sequenced murine rodents to provide both a general resource for future comparative genomic studies within this important group as well as a time-calibrated phylogeny to frame an in-depth analysis of phylogenetic discordance across a subset of murine whole genomes (see below). We combined our seven recently sequenced genomes with nine publicly available murine genomes as well as the genomes of two non-murine rodents, the great gerbil (*Rhombomys opimus*; (Nilsson, et al. 2020) and the Siberian hamster (*Phodopus sungorus*; (Moore, et al. 2022) as outgroups. We extracted UCEs from each species, plus 1000 flanking bases from each side of the element using the protocols for harvesting loci from genomes and the *M. musculus* UCE probe set provided with phyluce v1.7.1 (Faircloth, et al. 2012; Faircloth 2016). In total, we recovered 2,632 unique UCE loci, though not all UCE loci were found in all taxa (Table S1).

We brought the extracted UCE sequences for each species into a consistent orientation using MAFFT v7 (Katoh and Standley 2013) and then aligned them using FSA (Bradley, et al. 2009) with the default settings. We trimmed UCE alignments with TrimAl (Capella-Gutierrez, et

528 al. 2009) with a gap threshold of 0.5 and otherwise default parameters. We performed alignment
529 quality checks using AMAS (Borowiec 2016). We processed all alignments in parallel with GNU
530 Parallel (Tange 2018).
531
532 *Species tree reconstruction from UCEs*

533 We constructed a species-level rodent phylogeny with two approaches. First, using the alignments
534 of all UCEs found in four or more taxa (2,632), we reconstructed a maximum-likelihood (ML)
535 species tree with IQ-TREE v2.2.1 (Minh, et al. 2020b). Each UCE alignment was concatenated
536 and partitioned (Chernomor, et al. 2016) such that optimal substitution models were inferred for
537 individual UCE loci with ModelFinder (Kalyaanamoorthy, et al. 2017). We also reconstructed
538 individual gene trees for each UCE alignment. For all IQ-TREE runs (concatenated or individual
539 loci), we assessed branch support with ultrafast bootstrap approximation (UFBoot) (Hoang, et al.
540 2018) and the corrected approximate likelihood ratio test (SH-aLRT) (Guindon, et al. 2010). We
541 collapsed branches in each UCE tree exhibiting less than 10% approximated bootstrap support
542 using the nw_ed function from Newick Utilities (Junier and Zdobnov 2010). We used these trees
543 as input to the quartet summary method ASTRAL-III v5.7.8 (Zhang, et al. 2018) to infer a species
544 tree. We generated visualizations of phylogenies with R v4.1.1 (R Core Team 2021) using phytools
545 v1.9-16 (Revell 2012) and the ggtree package v3.14 (Yu, et al. 2017; Yu 2020) and its imported
546 functions from ape v5.0 (Paradis and Schliep 2019) and treeio v1.16.2 (Wang, et al. 2020).
547   We then used two methods to assess phylogenetic discordance across the reconstructed
548 species tree. First, we calculated site and gene concordance factors (sCF and gCF) with IQ-TREE
549 2 (Minh, et al. 2020a; Minh, et al. 2020b) to assess levels of phylogenetic discordance between the
550 inferred UCE trees and the concatenated species tree. gCF is calculated for each branch in the
551 species tree as the proportion of UCE trees in which that branch also appears (Baum 2007). sCF
552 represents the proportion of alignment sites concordant with a given species tree branch in a
553 randomized subset of quartets of taxa (Minh, et al. 2020a). We visualized gCF and sCF (Lanfear
554 2018) for each branch in each species tree using methods in R v4.3.0 (Lanfear 2018; R Core Team
555 2021). Next, we used PhyParts (Smith, et al. 2015b) to identify topological conflict between the
556 UCE trees and the species tree from ASTRAL-III. For this analysis, we rooted all trees with
557 *Phodopus sungorus* as the outgroup using the nw_reroot function in the Newick Utilities (Junier
558 and Zdobnov 2010) package and excluded 204 UCE trees that did not contain the outgroup.
559
560 *Divergence time estimation*

561 We used IQ-TREE 2's (Minh, et al. 2020b) implementation of least square dating to estimate
562 branch lengths of our species trees in units of absolute time (To, et al. 2016). To improve
563 divergence-time estimation, we used SortaDate (Smith, et al. 2018) to identify a set of 100 UCE
564 loci that exhibit highly clocklike behavior and minimized topological conflict with the
565 concatenated species tree. We applied four node age calibrations (Table S3) as described in
566 Kimura, et al. (2015) and Aghova, et al. (2018). The origin of core Murinae (Node E) was

15

567 constrained to between 11.1 and 12.3 Ma, following Kimura, et al. (2015). Maximum ages were
568 set for Otomyini+Arvicanthini (9.2 Ma, Kimura, et al. 2015), *Apodemus* (9.6 Ma, Daxner-Höck
569 2002), and *Mus* (8.0 Ma, Kimura, et al. 2013). Branch lengths were resampled 100 times to produce
570 confidence intervals.
571
572 *Genome window-based phylogenetic analysis*

573 For the second part of our work, we wanted to quantitatively infer phylogenetic discordance across
574 a subset of the murine genomes used to infer the species tree and relate that discordance to other
575 features of the genome, such as recombination rate, proximity to genes, and rates of molecular
576 evolution. To assess the distribution of phylogenetic discordance across rodent genomes, we
577 limited subsequent analyses to *M. musculus* and the pseudo-assemblies (see above) of six of the
578 genomes (*Mastomys natalensis*, *Hylomyscus alleni*, *Praomys delectorum*, *Rhabdomys dilectus*,
579 *Grammomys dolichurus*, and *Rhynchomys soricoides*). *Otomys typus* was excluded from these
580 analyses due to the inadequacy of the library outlined above.
581　　　　We partitioned these genomes into 10 kilobase (kb) windows based on the coordinates in
582 the reference *M. musculus* genome (mm10; Mouse Genome Sequencing, et al. 2002) using
583 bedtools makewindows (Quinlan and Hall 2010). These coordinates were converted between the
584 reference and the consensus sequence for each genome using liftOver (Hinrichs, et al. 2006). Note
585 that this method assumes both collinearity of all genomes and similar karyotypes (see Discussion).
586 We then removed windows from the subsequent analyses if (1) 50% or more of the window
587 overlapped with repeat regions from the *M. musculus* reference RepeatMasker (Smit, et al. 2013-
588 2015) file downloaded from the UCSC Genome Browser's table browser (Hinrichs, et al. 2006)
589 or (2) 50% or more of the window contained missing data in three or more samples. Overlaps with
590 repeat regions were determined with bedtools coverage (Quinlan and Hall 2010). We then aligned
591 the 10kb windows with MAFFT (Katoh and Standley 2013), trimmed alignments with trimAl
592 (Capella-Gutierrez, et al. 2009), and inferred phylogenies for each with IQ-TREE 2 (Minh, et al.
593 2020b) which uses ModelFinder to determine the best substitution model for each window
594 (Kalyaanamoorthy, et al. 2017).
595　　　　To assess patterns of tree similarity between windows on the same chromosome, we used
596 the weighted Robinson-Foulds (wRF) (Robinson and Foulds 1981; Böcker, et al. 2013) distance
597 measure implemented in the phangorn library (Schliep 2011) in R (R Core Team 2021), which
598 compares two trees by finding clades or splits present in one tree but not the other weighted by the
599 missing branch length in each tree for each mismatch and differences in branch length between the
600 co-occurring branches in both trees (Robinson and Foulds 1979). Consequently, the resulting
601 measure of wRF is in units of branch length (i.e., expected number of substitutions per site for
602 maximum likelihood trees). We compared wRF between trees from windows on the same
603 chromosome to characterize (1) heterogeneity in patterns discordance along the chromosome and
604 (2) whether tree similarity is correlated with distance between windows. For the second question,
605 we sampled every window on a chromosome at increasing distance (in 10kb windows) until the
606 distribution of wRF scores for all pairs of windows at that distance was not significantly different

607　(Wilcox test, p > 0.01) than that of a sample of 12,000 measures of wRF between randomly
608　selected trees on different chromosomes. We selected 12,000 as the random sample size because
609　it roughly matched the number of windows on the largest chromosome (chromosome 1, n =
610　12,113). We used Snakemake 7 (Mölder, et al. 2021) to compute window alignments and trees in
611　parallel.

612

613　*Whole genome alignment between mouse and rat*

614

615　To assess how un-accounted for large-scale structural variation may impact our conclusions, we
616　compared the reference mouse and rat genomes. We used minimap2 (Li 2018) to align the mouse
617　(mm10) and rat (rnor6) (Gibbs, et al. 2004) genomes to assess the impact of structural variation
618　that spans the divergence of our subset of species used in the discordance analyses. We
619　downloaded the rat reference genome (rnor6) from the UCSC genome browser and for both
620　genomes removed the Y chromosome and all smaller unplaced scaffolds. We then used minimap2
621　in whole genome alignment mode (-x asm20) to generate a pairwise alignment file from which we
622　calculated alignment segment sizes and the distances between alignment segments. We visualized
623　the alignment as a dot plot using the pafr package in R (https://github.com/dwinter/pafr).

624

625　*Recombination rate and functional annotation*

626　We retrieved 10,205 genetic markers generated from a large heterogenous stock of outbred mice
627　(Shifman, et al. 2006; Cox, et al. 2009) to assess whether phylogenetic discordance along
628　chromosomes was correlated with mouse recombination rates. We converted the physical
629　coordinates of these markers from build 37 (mm9) to build 38 (mm10) of the *M. musculus* genome
630　using liftOver (Hinrichs, et al. 2006). We then partitioned the markers into 5Mb windows and
631　estimated local recombination rates defined as the slope of the correlation between the location on
632　the *M. musculus* genetic and physical maps for all markers in the window (White, et al. 2009;
633　Kartje, et al. 2020). Within each 5Mb window, we calculated wRF distances between the first 10kb
634　window and every other 10kb window.
635　　　We also compared the chromosome-wide wRF distances to those based on phylogenies
636　from regions around several types of adjacent to genomic features. We retrieved coordinates from
637　25,753 protein coding genes annotated in *M. musculus* from Ensembl (release 99; Cunningham, et
638　al. 2022), all 3,129 UCEs from the *M. musculus* UCE probe set provided with PHYLUCE
639　(Faircloth, et al. 2012; Faircloth 2016), and 9,865 recombination hotspots from Smagulova, et al.
640　(2011). The recombination hotspot coordinates were converted between build 37 and build 38
641　using the liftOver tool (Hinrichs, et al. 2006). For each feature, the starting window was the 10kb
642　window containing the feature's midpoint coordinate. We then calculated wRF between this
643　window and all windows within 5Mb in either direction and for each chromosome compared the
644　slope and wRF distance of windows adjacent to the feature with the same metrics for the whole
645　chromosome. We compared distributions of these measures for each genomic feature with an
646　ANOVA　(aov(feature.measure　~　feature.label))　followed　by　Tukey's　range　test

647   (TukeyHSD(anova.result)) to assess differences in means, as implemented in R v4.1.1 (R Core
648   Team 2021).

649   *Molecular evolution*

650   To test how tree misspecification affects common model-based analyses of molecular evolution,
651   we retrieved 22,261 coding sequences from *M. musculus* using the longest coding transcript of
652   each gene. Coding coordinates from the *M. musculus* coding sequences were transposed to the new
653   assemblies via liftOver (Hinrichs, et al. 2006) and sequences retrieved with bedtools getfasta
654   (Quinlan and Hall 2010). We recovered 17,216 genes that were present in all seven species. Using
655   MACSE (Ranwez, et al. 2018), we trimmed non-homologous regions from each ortholog using
656   trimNonHomologousFragments, aligned the orthologs using alignSequences, and trimmed the
657   aligned sequences with trimAlignment to remove unaligned flanking regions. Finally, we manually
658   filtered the alignments using the following (non-mutually exclusive) criteria: 3,368 alignments
659   were removed during filtering for gapped sites, 3,132 alignments had a premature stop codon in at
660   least one species, 1,571 alignments had only three or fewer unique sequences among the seven
661   species, and 78 alignments were shorter than 100 bp. After filtering, 12,559 total alignments for
662   tree reconstruction and inference of selection.

663   We then used IQ-TREE 2 (Minh, et al. 2020b) to reconstruct a single species tree from
664   concatenation of all gene alignments, as well as gene-trees for each individual alignment. This
665   species tree from coding regions matches the topologies of these species inferred by concatenation
666   of UCEs in the previous section. Next we ran several tests that use both coding alignments and a
667   tree to infer positive selection: PAML's M1a vs. M2a test (Yang 2007), HyPhy's aBSREL model
668   (Smith, et al. 2015a), and HyPhy's BUSTED model (Murrell, et al. 2015). We ran each test twice
669   on each gene, once using the species tree derived from concatenated data, and once using the tree
670   estimated for that gene. For the HyPhy models, no target branch was selected, meaning all branches
671   in the input phylogeny were tested.

672   The end point of each of these three tests is a p-value, which lets us assess whether a model
673   that allows for positively selected sites fits better than a model that does not. For M1a vs. M2a, we
674   obtained the p-value manually by first performing a likelihood ratio test to determine genes under
675   selection by calculating $2 * (lnl\ M1a - lnl\ M2a)$. The p-value of this likelihood ratio is then
676   retrieved from a one-tailed chi-square distribution with two degrees of freedom (Yang 2007). For
677   BUSTED and aBSREL, p-values are computed automatically during the test using similar
678   likelihood ratios. For the M1a vs. M2a and BUSTED tests, a single p-value is computed for each
679   gene. P-values were adjusted by correcting for false discovery rates (Benjamini and Hochberg
680   1995; Yekutieli and Benjamini 1999) using the "fdr" method in the p.adjust() function in R (R
681   Core Team 2021) and we categorized a gene as being positively selected if its adjusted p-value
682   was < 0.01. For the aBSREL test, a p-value is generated for each branch in the input gene tree.
683   aBSREL corrects for multiple testing internally across branches using the Holm-Bonferroni
684   procedure (Holm 1979; Pond, et al. 2005). We further correct the p-values across genes with the
685   Bonferroni method and classify a gene as having experienced positive selection if one or more

686 branches has a p-value < 0.01 after all corrections. We used Snakemake 7 (Mölder, et al. 2021) to
687 compute coding alignments, trees, and selection tests in parallel.
688

689 **Data availability**

690 For the six previously assembled genomes (see Table S1), all raw reads and assemblies are
691 available as an NCBI BioProject (Accession Number PRJNA669840). The reads and assembly
692 for *Otomys* typus, pseudo-assemblies for the six other new samples, and locus alignments
693 (UCEs, genes, and genomic windows) are available on Dryad
694 (https://doi.org/10.5061/dryad.866t1g1wq). All code and summary data for this project are
695 deposited on github (https://github.com/gwct/murine-discordance).

696

717

718

19

Tables

Table 1. Incidence where a single species tree does not match the gene tree expectation in three different tests for positive selection, either not detecting positive selection when it is inferred using the gene tree (Undetected selection) or by detecting positive selection that is not inferred when using the gene tree (Newly detected selection).

Test	Undetected selection	Newly detected selection
BUSTED	0.45%	28.10%
aBSREL	0.41%	10.60%
M1a vs. M2a	2.66%	3.20%

727
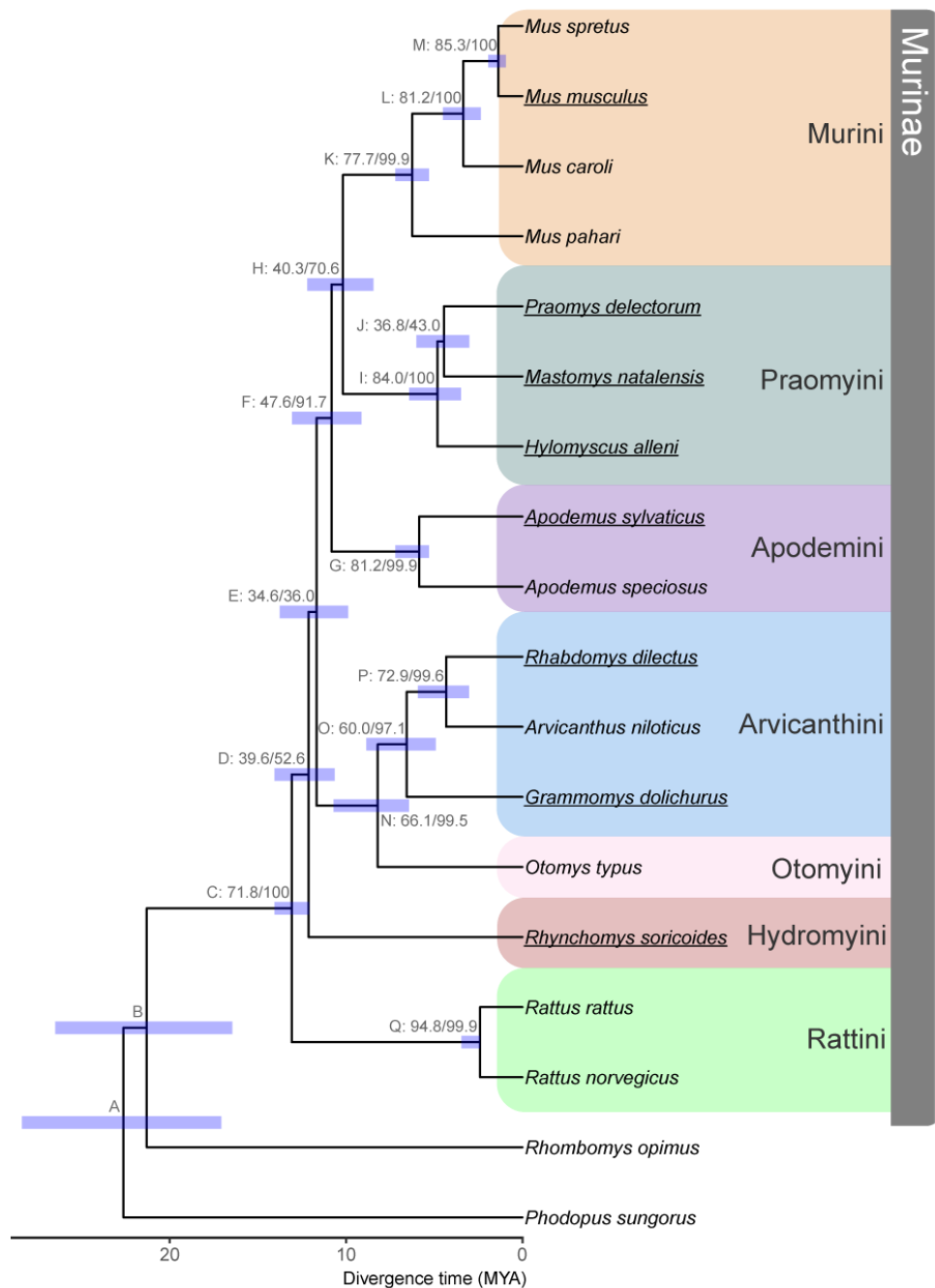
Figure 1. Species trees inferred from concatenation of ultra-conserved elements (UCEs) from 18
rodent species. Internal nodes are labeled by a letter identifier referenced in the text and site and
gene concordance factors (*i.e.*, Label: sCF/gCF) as well as a bar indicating the confidence interval
for divergence time estimation. Ultrafast bootstrap/SH-aLRT values were all 100. Bottom scale
represents time in millions of years before present. Fossil calibrations are described in Tables S2

733　and S3. Tribes within sub-family Murinae are highlighted on the right following the classifications
734　used by Lecompte, et al. (2008). Genomes used for the genome-wide phylogenetic discordance
735　analyses are underlined.

736

737   **Figure 2**

A

B

C
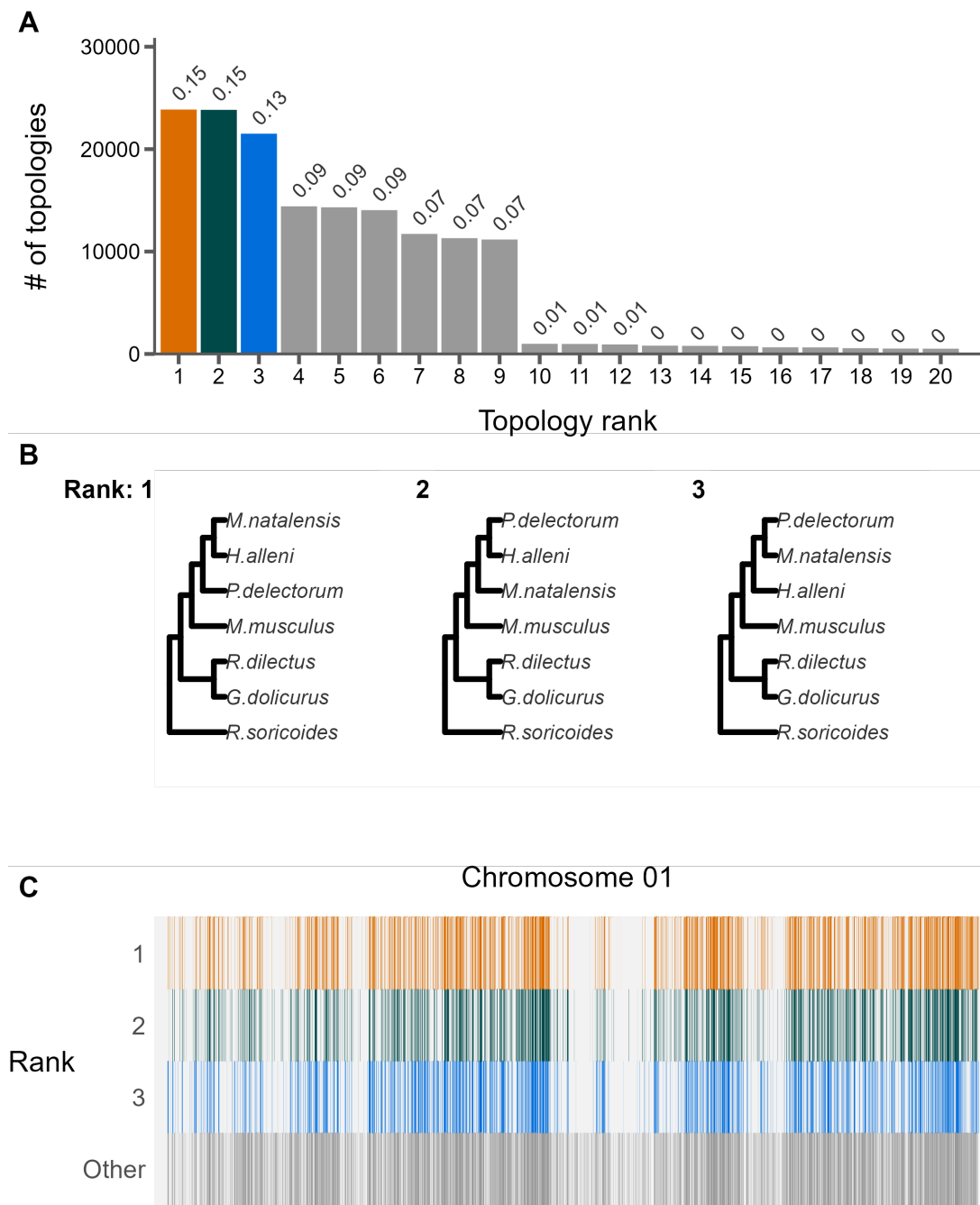
738

739   **Figure 2.** The landscape and profile of phylogenetic discordance across non-overlapping 10kb
740   windows in murine genomes. A) Distribution of the 20 most frequent topologies recovered across
741   all windows. Numbers above bars indicate proportion of each topology. B) The top three
742   topologies recovered across all chromosomes 1. C) Distribution of the topologies recovered along

chromosome 1. The x-axis is scaled to the length of the chromosome and each vertical bar represents one 10kb window. The three most frequent topologies occupy the first three rows while all other topologies are shown in the bottom row. See Supplemental File S1 for individual chromosome plots.

747 **Figure 3**

748
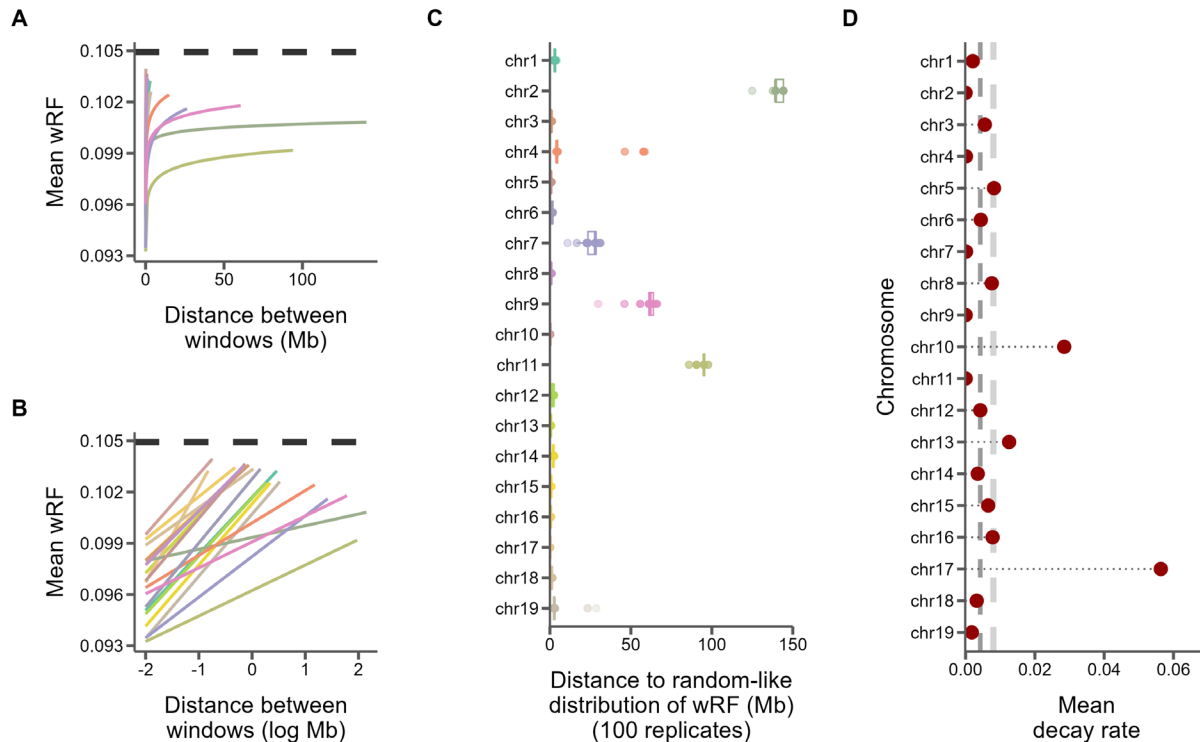
Figure 3. Similarity between 10kb windows decays as genomic distance between windows increases. A) The log fit to the mean of distributions of weighted Robinson-Foulds distances between trees of windows at increasing genomic distance (10kb steps). Each line represents one chromosome. B) The same, but on a log scale with a linear fit. C) For every window on each chromosome, the genomic distance between windows at which tree distance becomes random for 100 replicates of random window selection. D) Points represent the slopes of the correlation between genomic distance and tree distance (lines from panel B), which is the rate at which tree similarity decays across the genome. Dark grey dashed line is median slope and light grey dashed line is mean.

758

759   **Figure 4**

760
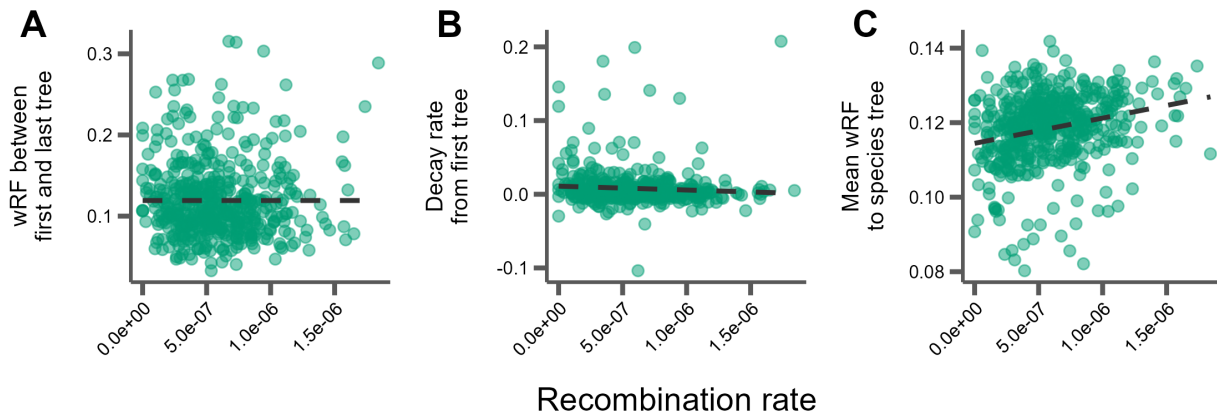
Figure 4. Correlations between tree similarity and recombination rate in 5 Mb windows. A) Tree
similarity as measured by the weighted Robinson-Foulds distance between the first and last 10 kb
windows within the 5 Mb window. B) The slopes of the linear correlation between the weighted
Robinson-Foulds distances between the first 10 kb window and every other 10 kb window within
a 5 Mb window represent the rate at which tree similarity decays over each 5 Mb window. C) The
mean wRF of all 10 kb window trees within each 5Mb window compared to the species tree.

767
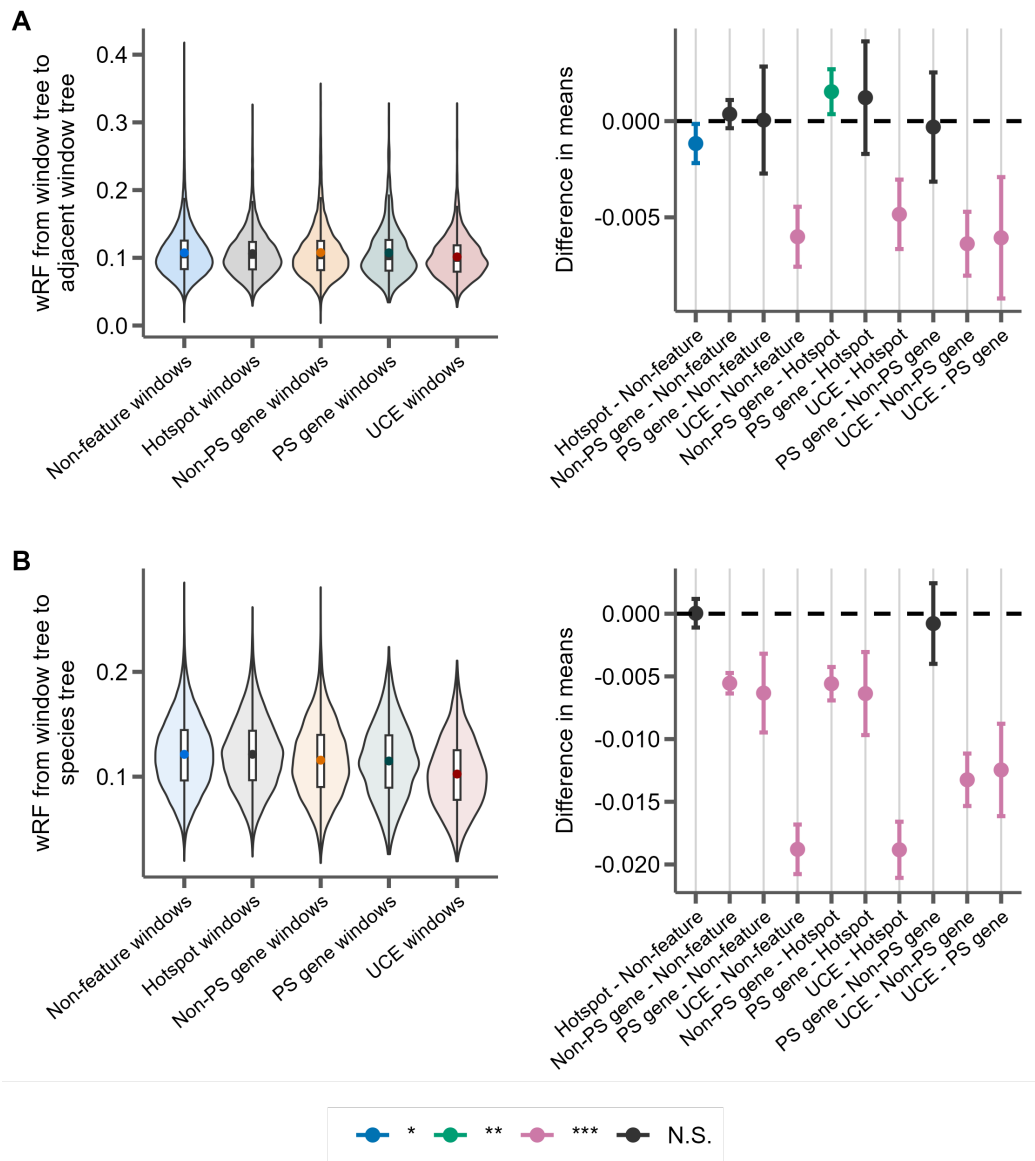
Figure 5

Figure 5. Distributions of weighted Robinson-Foulds distance from trees constructed from 10kb windows either centered on recombination hotspots (Hotspot), protein-coding genes without evidence for positive selection (Non-PS genes), protein coding genes with evidence for positive selection (PS genes), UCEs, or containing none of these features (Non-feature). For each panel, the left portion shows the distributions of the measure for each feature type and the right panel shows the differences in means for each pairwise comparison of features with significance assessed with Tukey's range test. The labels on the x-axis indicate the feature pairs being compared, with the first feature being the reference (*i.e.* points above 0 indicate this feature has a higher mean). *P*-value thresholds: * < 0.05, ** < 0.01, *** <0.001. A) The phylogenetic similarity of windows

779   immediately adjacent to feature windows. B) The phylogenetic similarity between the species tree
780   inferred from protein-coding gene trees and the feature window.

781

782   **Figure 6**
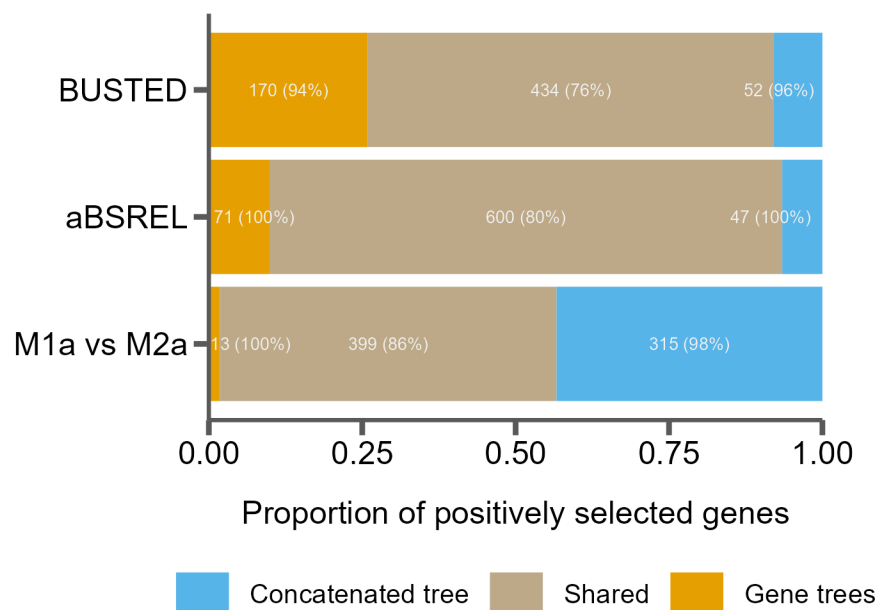
Figure 6. The proportion of genes inferred to be under positive selection for three tests using either a single species tree (concatenated tree) or individual gene trees, as well as those found in both cases (shared). Numbers in the bars indicate raw counts, and percentages indicate the percent of genes in that category that are discordant from the species tree.

References

Aghova T, Kimura Y, Bryja J, Dobigny G, Granjon L, Kergoat GJ. 2018. Fossils know it best: Using a new set of fossil calibrations to improve the temporal phylogenetic framework of murid rodents (Rodentia: Muridae). Mol Phylogenet Evol 128:98-111.

Alda F, Ludt WB, Elias DJ, McMahan CD, Chakrabarty P. 2021. Comparing Ultraconserved Elements and Exons for Phylogenomic Analyses of Middle American Cichlids: When Data Agree to Disagree. Genome Biol Evol 13:evab161.

Alexander AM, Su YC, Oliveros CH, Olson KV, Travers SL, Brown RM. 2017. Genomic data reveals potential for hybridization, introgression, and incomplete lineage sorting to confound phylogenetic relationships in an adaptive radiation of narrow-mouth frogs. Evolution 71:475-488.

Avise JC, Robinson TJ. 2008. Hemiplasy: a new term in the lexicon of phylogenetics. Syst Biol 57:503-507.

Baudat F, Buard J, Grey C, Fledel-Alon A, Ober C, Przeworski M, Coop G, de Massy B. 2010. PRDM9 is a major determinant of meiotic recombination hotspots in humans and mice. Science 327:836-840.

Baum DA. 2007. Concordance trees, concordance factors, and the exploration of reticulate genealogy. TAXON 56:417-426.

Benjamini Y, Hochberg Y. 1995. Controlling the false discovery rate: a practical and powerful approach to multiple testing. Journal of the Royal statistical society: series B (Methodological) 57:289-300.

Bloom BH. 1970. Space/time trade-offs in hash coding with allowable errors. Commun. ACM 13:422–426.

Böcker S, Canzar S, Gunnar WK. 2013. The Generalized Robinson-Foulds Metric. In: Darling A, Stoye J, editors. Algorithms in Bioinformatics. Berlin, Heidelberg: Springer.

Bolger AM, Lohse M, Usadel B. 2014. Trimmomatic: a flexible trimmer for Illumina sequence data. Bioinformatics 30:2114-2120.

Borowiec ML. 2016. AMAS: a fast tool for alignment manipulation and computing of summary statistics. PeerJ 4:e1660.

829

830 Bradley RK, Roberts A, Smoot M, Juvekar S, Do J, Dewey C, Holmes I, Pachter L. 2009. Fast
831 statistical alignment. PLoS Comput Biol 5:e1000392.

832

833 Capella-Gutierrez S, Silla-Martinez JM, Gabaldon T. 2009. trimAl: a tool for automated alignment
834 trimming in large-scale phylogenetic analyses. Bioinformatics 25:1972-1973.

835

836 Carbone L, Harris RA, Gnerre S, Veeramah KR, Lorente-Galdos B, Huddleston J, Meyer TJ,
837 Herrero J, Roos C, Aken B, et al. 2014. Gibbon genome and the fast karyotype evolution of small
838 apes. Nature 513:195-201.

839

840 Chan KO, Hutter CR, Wood PL, Jr., Grismer LL, Brown RM. 2020. Target-capture phylogenomics
841 provide insights on gene and species tree discordances in Old World treefrogs (Anura:
842 Rhacophoridae). Proc Biol Sci 287:20202102.

843

844 Charlesworth B, Morgan MT, Charlesworth D. 1993. The effect of deleterious mutations on
845 neutral molecular variation. Genetics 134:1289-1303.

846

847 Chernomor O, von Haeseler A, Minh BQ. 2016. Terrace Aware Data Structure for Phylogenomic
848 Inference from Supermatrices. Syst Biol 65:997-1008.

849

850 Christmas MJ, Kaplow IM, Genereux DP, Dong MX, Hughes GM, Li X, Sullivan PF, Hindle AG,
851 Andrews G, Armstrong JC, et al. 2023. Evolutionary constraint and innovation across hundreds of
852 placental mammals. Science 380:eabn3943.

853

854 Cox A, Ackert-Bicknell CL, Dumont BL, Ding Y, Bell JT, Brockmann GA, Wergedal JE, Bult C,
855 Paigen B, Flint J, et al. 2009. A new standard genetic map for the laboratory mouse. Genetics
856 182:1335-1344.

857

858 Cunningham F, Allen JE, Allen J, Alvarez-Jarreta J, Amode MR, Armean IM, Austine-Orimoloye
859 O, Azov AG, Barnes I, Bennett R, et al. 2022. Ensembl 2022. Nucleic Acids Res 50:D988-D995.

860

861 Danecek P, Bonfield JK, Liddle J, Marshall J, Ohan V, Pollard MO, Whitwham A, Keane T,
862 McCarthy SA, Davies RM, Li H. 2021. Twelve years of SAMtools and BCFtools. Gigascience
863 10:giab008.

864

865 Dapper AL, Payseur BA. 2017. Connecting theory and data to understand recombination rate
866 evolution. Philos Trans R Soc Lond B Biol Sci 372.

867

868 Daxner-Höck G. 2002. Cricetodon meini and other rodents from Mühlbach and Grund, Lower
869 Austria (Middle Miocene, late MN5). Annalen des Naturhistorischen Museums in Wien. Serie A
870 für Mineralogie und Petrographie, Geologie und Paläontologie, Anthropologie und
871 Prähistorie:267-291.

872

873 Degnan JH, Rosenberg NA. 2006. Discordance of species trees with their most likely gene trees.
874 PLoS Genet 2:e68.

875

876 Edwards SV. 2009. Is a new and general theory of molecular systematics emerging? Evolution
877 63:1-19.

878

879 Faircloth BC. 2013. illumiprocessor: a trimmomatic wrapper for parallel adapter and quality
880 trimming.

881

882 Faircloth BC. 2016. PHYLUCE is a software package for the analysis of conserved genomic loci.
883 Bioinformatics 32:786-788.

884

885 Faircloth BC, McCormack JE, Crawford NG, Harvey MG, Brumfield RT, Glenn TC. 2012.
886 Ultraconserved elements anchor thousands of genetic markers spanning multiple evolutionary
887 timescales. Syst Biol 61:717-726.

888

889 Feng S, Bai M, Rivas-Gonzalez I, Li C, Liu S, Tong Y, Yang H, Chen G, Xie D, Sears KE, et al.
890 2022. Incomplete lineage sorting and phenotypic evolution in marsupials. Cell 185:1646-1660
891 e1618.

892

893 Ferreira MS, Jones MR, Callahan CM, Farelo L, Tolesa Z, Suchentrunk F, Boursot P, Mills LS,
894 Alves PC, Good JM, Melo-Ferreira J. 2021. The Legacy of Recurrent Introgression during the
895 Radiation of Hares. Syst Biol 70:593-607.

896

897 Foley NM, Harris AJ, Bredemeyer KR, Ruedi M, Puechmaille SJ, Teeling EC, Criscitiello MF,
898 Murphy WJ. 2024. Karyotypic stasis and swarming influenced the evolution of viral tolerance in
899 a species-rich bat radiation. Cell Genom 4:100482.

900

901 Foley NM, Mason VC, Harris AJ, Bredemeyer KR, Damas J, Lewin HA, Eizirik E, Gatesy J,
902 Karlsson EK, Lindblad-Toh K, et al. 2023. A genomic timescale for placental mammal evolution.
903 Science 380:eabl8189.

904

905 Fontaine MC, Pease JB, Steele A, Waterhouse RM, Neafsey DE, Sharakhov IV, Jiang X, Hall AB,
906 Catteruccia F, Kakani E, et al. 2015. Mosquito genomics. Extensive introgression in a malaria
907 vector species complex revealed by phylogenomics. Science 347:1258524.

908
909 Foote AD, Liu Y, Thomas GW, Vinar T, Alfoldi J, Deng J, Dugan S, van Elk CE, Hunter ME,
910 Joshi V, et al. 2015. Convergent evolution of the genomes of marine mammals. Nat Genet 47:272-
911 275.

912
913 Gable SM, Byars MI, Literman R, Tollis M. 2022. A Genomic Perspective on the Evolutionary
914 Diversification of Turtles. Syst Biol 71:1331-1347.

915
916 Gibbs RA, Weinstock GM, Metzker ML, Muzny DM, Sodergren EJ, Scherer S, Scott G, Steffen
917 D, Worley KC, Burch PE, et al. 2004. Genome sequence of the Brown Norway rat yields insights
918 into mammalian evolution. Nature 428:493-521.

919
920 Good JM, Wiebe V, Albert FW, Burbano HA, Kircher M, Green RE, Halbwax M, Andre C,
921 Atencia R, Fischer A, Paabo S. 2013. Comparative population genomics of the ejaculate in humans
922 and the great apes. Mol Biol Evol 30:964-976.

923
924 Green RE, Krause J, Briggs AW, Maricic T, Stenzel U, Kircher M, Patterson N, Li H, Zhai W,
925 Fritz MH, et al. 2010. A draft sequence of the Neandertal genome. Science 328:710-722.

926
927 Guindon S, Dufayard JF, Lefort V, Anisimova M, Hordijk W, Gascuel O. 2010. New algorithms
928 and methods to estimate maximum-likelihood phylogenies: assessing the performance of PhyML
929 3.0. Syst Biol 59:307-321.

930
931 Hahn MW, Nakhleh L. 2016. Irrational exuberance for resolved species trees. Evolution 70:7-17.

932
933 He B, Zhao Y, Su C, Lin G, Wang Y, Li L, Ma J, Yang Q, Hao J. 2023. Phylogenomics reveal
934 extensive phylogenetic discordance due to incomplete lineage sorting following the rapid radiation
935 of alpine butterflies (Papilionidae: Parnassius). Syst Entomol.

936
937 Hibbins MS, Breithaupt LC, Hahn MW. 2023. Phylogenomic comparative methods: Accurate
938 evolutionary inferences in the presence of gene tree discordance. Proc Natl Acad Sci U S A
939 120:e2220389120.

940
941 Hinrichs AS, Karolchik D, Baertsch R, Barber GP, Bejerano G, Clawson H, Diekhans M, Furey
942 TS, Harte RA, Hsu F, et al. 2006. The UCSC Genome Browser Database: update 2006. Nucleic
943 Acids Res 34:D590-598.

944

945 Hoang DT, Chernomor O, von Haeseler A, Minh BQ, Vinh LS. 2018. UFBoot2: Improving the
946 Ultrafast Bootstrap Approximation. Mol Biol Evol 35:518-522.

947

948 Hobolth A, Christensen OF, Mailund T, Schierup MH. 2007. Genomic relationships and speciation
949 times of human, chimpanzee, and gorilla inferred from a coalescent hidden Markov model. PLoS
950 Genet 3:e7.

951

952 Holm S. 1979. A simple sequentially rejective multiple test procedure. Scandinavian journal of
953 statistics:65-70.

954

955 Hu Z, Sackton TB, Edwards SV, Liu JS. 2019. Bayesian Detection of Convergent Rate Changes
956 of Conserved Noncoding Elements on Phylogenetic Trees. Mol Biol Evol 36:1086-1100.

957

958 Hudson RR. 1983. Testing the Constant-Rate Neutral Allele Model with Protein Sequence Data.
959 Evolution 37:203-217.

960

961 Hudson RR, Kaplan NL. 1988. The coalescent process in models with selection and
962 recombination. Genetics 120:831-840.

963

964 Hudson RR, Kaplan NL. 1995. Deleterious background selection with recombination. Genetics
965 141:1605-1617.

966

967 Huson DH, Klöpper T, Lockhart PJ, Steel MA. 2005. Reconstruction of Reticulate Networks from
968 Gene Trees. In: Miyano S, Mesirov J, Kasif S, Istrail S, Pevzner PA, Waterman M, editors.
969 Research in Computational Molecular Biology. RECOMB 2005. Lecture Notes in Computer
970 Science: Springer, Berlin, Heidelberg.

971

972 Jackman SD, Vandervalk BP, Mohamadi H, Chu J, Yeo S, Hammond SA, Jahesh G, Khan H,
973 Coombe L, Warren RL, Birol I. 2017. ABySS 2.0: resource-efficient assembly of large genomes
974 using a Bloom filter. Genome Res 27:768-777.

975

976 Jarvis ED, Mirarab S, Aberer AJ, Li B, Houde P, Li C, Ho SY, Faircloth BC, Nabholz B, Howard
977 JT, et al. 2014. Whole-genome analyses resolve early branches in the tree of life of modern birds.
978 Science 346:1320-1331.

979

980 Jensen-Seaman MI, Furey TS, Payseur BA, Lu Y, Roskin KM, Chen CF, Thomas MA, Haussler
981 D, Jacob HJ. 2004. Comparative recombination rates in the rat, mouse, and human genomes.
982 Genome Res 14:528-538.

983

984 Johri P, Aquadro CF, Beaumont M, Charlesworth B, Excoffier L, Eyre-Walker A, Keightley PD,
985 Lynch M, McVean G, Payseur BA, et al. 2022. Recommendations for improving statistical
986 inference in population genomics. PLoS Biol 20:e3001669.

987

988 Jones MR, Mills LS, Alves PC, Callahan CM, Alves JM, Lafferty DJR, Jiggins FM, Jensen JD,
989 Melo-Ferreira J, Good JM. 2018. Adaptive introgression underlies polymorphic seasonal
990 camouflage in snowshoe hares. Science 360:1355-1358.

991

992 Junier T, Zdobnov EM. 2010. The Newick utilities: high-throughput phylogenetic tree processing
993 in the UNIX shell. Bioinformatics 26:1669-1670.

994

995 Kalyaanamoorthy S, Minh BQ, Wong TKF, von Haeseler A, Jermiin LS. 2017. ModelFinder: fast
996 model selection for accurate phylogenetic estimates. Nat Methods 14:587-589.

997

998 Kaplan NL, Hudson RR, Langley CH. 1989. The "hitchhiking effect" revisited. Genetics 123:887-
999 899.

1000

1001 Kartje ME, Jing P, Payseur BA. 2020. Weak Correlation between Nucleotide Variation and
1002 Recombination Rate across the House Mouse Genome. Genome Biol Evol 12:293-299.

1003

1004 Katoh K, Standley DM. 2013. MAFFT multiple sequence alignment software version 7:
1005 improvements in performance and usability. Mol Biol Evol 30:772-780.

1006

1007 Katzman S, Kern AD, Bejerano G, Fewell G, Fulton L, Wilson RK, Salama SR, Haussler D. 2007.
1008 Human genome ultraconserved elements are ultraselected. Science 317:915.

1009

1010 Keane TM, Wong K, Adams DJ, Flint J, Reymond A, Yalcin B. 2014. Identification of structural
1011 variation in mouse genomes. Front Genet 5:192.

1012

1013 Kimura Y, Hawkins MT, McDonough MM, Jacobs LL, Flynn LJ. 2015. Corrected placement of
1014 Mus-Rattus fossil calibration forces precision in the molecular tree of rodents. Sci Rep 5:14444.

1015

1016 Kimura Y, Jacobs LL, Cerling TE, Uno KT, Ferguson KM, Flynn LJ, Patnaik R. 2013. Fossil mice
1017 and rats show isotopic evidence of niche partitioning and change in dental ecomorphology related
1018 to dietary shift in Late Miocene of Pakistan. PLoS One 8:e69308.

1019

Kong A, Gudbjartsson DF, Sainz J, Jonsdottir GM, Gudjonsson SA, Richardsson B, Sigurdardottir S, Barnard J, Hallbeck B, Masson G, et al. 2002. A high-resolution recombination map of the human genome. Nat Genet 31:241-247.

Kowalczyk A, Meyer WK, Partha R, Mao W, Clark NL, Chikina M. 2019. RERconverge: an R package for associating evolutionary rates with convergent traits. Bioinformatics 35:4815-4817.

Kulathinal RJ, Stevison LS, Noor MA. 2009. The genomics of speciation in Drosophila: diversity, divergence, and introgression estimated using low-coverage genome sequencing. PLoS Genet 5:e1000550.

Kumon T, Ma J, Akins RB, Stefanik D, Nordgren CE, Kim J, Levine MT, Lampson MA. 2021. Parallel pathways for recruiting effector proteins determine centromere drive and suppression. Cell 184:4904-4918 e4911.

Calculating and interpreting gene- and site-concordance factors in phylogenomics [Internet]. The Lanfear Lab @ ANU2018 September 20, 2021]. Available from: http://www.robertlanfear.com/blog/files/concordance_factors.html

Lecompte E, Aplin K, Denys C, Catzeflis F, Chades M, Chevret P. 2008. Phylogeny and biogeography of African Murinae based on mitochondrial and nuclear gene sequences, with a new tribal classification of the subfamily. BMC Evol Biol 8:199.

Lewontin RC, Birch LC. 1966. Hybridization as a Source of Variation for Adaptation to New Environments. Evolution 20:315-336.

Li H. 2013. Aligning sequence reads, clone sequences and assembly contigs with BWA-MEM. arXiv preprint arXiv:1303.3997.

Li H. 2018. Minimap2: pairwise alignment for nucleotide sequences. Bioinformatics 34:3094-3100.

Liu X, Wei F, Li M, Jiang X, Feng Z, Hu J. 2004. Molecular phylogeny and taxonomy of wood mice (genus Apodemus Kaup, 1829) based on complete mtDNA cytochrome b sequences, with emphasis on Chinese species. Mol Phylogenet Evol 33:1-15.

Lopes F, Oliveira LR, Kessler A, Beux Y, Crespo E, Cardenas-Alayza S, Majluf P, Sepulveda M, Brownell RL, Franco-Trecu V, et al. 2021. Phylogenomic Discordance in the Eared Seals is best

explained by Incomplete Lineage Sorting following Explosive Radiation in the Southern Hemisphere. Syst Biol 70:786-802.

Louca S, Pennell MW. 2020. Extant timetrees are consistent with a myriad of diversification histories. Nature 580:502-505.

Lundrigan BL, Jansa SA, Tucker PK. 2002. Phylogenetic relationships in the genus mus, based on paternally, maternally, and biparentally inherited characters. Syst Biol 51:410-431.

Maddison WP. 1997. Gene Trees in Species Trees. Systematic Biology 46:523-536.

Martin Y, Gerlach G, Schlotterer C, Meyer A. 2000. Molecular phylogeny of European muroid rodents based on complete cytochrome b sequences. Mol Phylogenet Evol 16:37-47.

Maynard Smith J, Haigh J. 1974. The hitch-hiking effect of a favourable gene. Genet Res 23:23-35.

McKenzie PF, Eaton DAR. 2020. The Multispecies Coalescent in Space and Time. bioRxiv:2020.2008.2002.233395.

Mendes FK, Fuentes-Gonzalez JA, Schraiber JG, Hahn MW. 2018. A multispecies coalescent model for quantitative traits. Elife 7:e36482.

Mendes FK, Hahn MW. 2016. Gene Tree Discordance Causes Apparent Substitution Rate Variation. Syst Biol 65:711-721.

Mendes FK, Hahn Y, Hahn MW. 2016. Gene Tree Discordance Can Generate Patterns of Diminishing Convergence over Time. Mol Biol Evol 33:3299-3307.

Mendes FK, Livera AP, Hahn MW. 2019. The perils of intralocus recombination for inferences of molecular convergence. Philos Trans R Soc Lond B Biol Sci 374:20180244.

Mikula O, Nicolas V, Šumbera R, Konečný A, Denys C, Verheyen E, Bryjová A, Lemmon AR, Lemmon EM, Bryja J. 2021. Nuclear phylogenomics, but not mitogenomics, resolves the most successful Late Miocene radiation of African mammals (Rodentia: Muridae: Arvicanthini). Molecular Phylogenetics and Evolution 157:107069.

1095   Minh BQ, Hahn MW, Lanfear R. 2020a. New Methods to Calculate Concordance Factors for
1096   Phylogenomic Datasets. Mol Biol Evol 37:2727-2733.

1097

1098   Minh BQ, Schmidt HA, Chernomor O, Schrempf D, Woodhams MD, von Haeseler A, Lanfear R.
1099   2020b. IQ-TREE 2: New Models and Efficient Methods for Phylogenetic Inference in the
1100   Genomic Era. Mol Biol Evol 37:1530-1534.

1101

1102   Mirarab S, Nakhleh L, Warnow T. 2021. Multispecies coalescent: theory and applications in
1103   phylogenetics. Annual Review of Ecology, Evolution, and Systematics 52:247-268.

1104

1105   Mölder F, Jablonski KP, Letcher B, Hall MB, Tomkins-Tinch CH, Sochat V, Forster J, Lee S,
1106   Twardziok SO, Kanitz A, et al. 2021. Sustainable data analysis with Snakemake. F1000Res 10:33.

1107

1108   Moore EC, Thomas GWC, Mortimer S, Kopania EEK, Hunnicutt KE, Clare-Salzler ZJ, Larson
1109   EL, Good JM. 2022. The Evolution of Widespread Recombination Suppression on the Dwarf
1110   Hamster (Phodopus) X Chromosome. Genome Biol Evol 14:evac080.

1111

1112   Mouse Genome Sequencing C, Waterston RH, Lindblad-Toh K, Birney E, Rogers J, Abril JF,
1113   Agarwal P, Agarwala R, Ainscough R, Alexandersson M, et al. 2002. Initial sequencing and
1114   comparative analysis of the mouse genome. Nature 420:520-562.

1115

1116   Murrell B, Weaver S, Smith MD, Wertheim JO, Murrell S, Aylward A, Eren K, Pollner T, Martin
1117   DP, Smith DM, et al. 2015. Gene-wide identification of episodic selection. Mol Biol Evol 32:1365-
1118   1371.

1119

1120   Nilsson P, Solbakken MH, Schmid BV, Orr RJS, Lv R, Cui Y, Song Y, Zhang Y, Baalsrud HT,
1121   Torresen OK, et al. 2020. The Genome of the Great Gerbil Reveals Species-Specific Duplication
1122   of an MHCII Gene. Genome Biol Evol 12:3832-3849.

1123

1124   Oliver JC. 2013. Microevolutionary processes generate phylogenomic discordance at ancient
1125   divergences. Evolution 67:1823-1830.

1126

1127   Pagès M, Fabre P-H, Chaval Y, Mortelliti A, Nicolas V, Wells K, Michaux JR, Lazzari V. 2016.
1128   Molecular phylogeny of South-East Asian arboreal murine rodents. Zoologica Scripta 45:349-364.

1129

1130   Pamilo P, Nei M. 1988. Relationships between gene trees and species trees. Mol Biol Evol 5:568-
1131   583.

1132

Paradis E, Schliep K. 2019. ape 5.0: an environment for modern phylogenetics and evolutionary analyses in R. Bioinformatics 35:526-528.

Partha R, Kowalczyk A, Clark NL, Chikina M. 2019. Robust Method for Detecting Convergent Shifts in Evolutionary Rates. Mol Biol Evol 36:1817-1830.

Pease JB, Haak DC, Hahn MW, Moyle LC. 2016. Phylogenomics Reveals Three Sources of Adaptive Variation during a Rapid Radiation. PLoS Biol 14:e1002379.

Pease JB, Hahn MW. 2013. More accurate phylogenies inferred from low-recombination regions in the presence of incomplete lineage sorting. Evolution 67:2376-2384.

Platt RN, 2nd, Vandewege MW, Ray DA. 2018. Mammalian transposable elements and their impacts on genome evolution. Chromosome Res 26:25-43.

Pollard KS, Hubisz MJ, Rosenbloom KR, Siepel A. 2010. Detection of nonneutral substitution rates on mammalian phylogenies. Genome Res 20:110-121.

Pond SL, Frost SD, Muse SV. 2005. HyPhy: hypothesis testing using phylogenies. Bioinformatics 21:676-679.

Poplin R, Ruano-Rubio V, DePristo MA, Fennell TJ, Carneiro MO, Auwera GAVd, Kling DE, Gauthier LD, Levy-Moonshine A, Roazen D, et al. 2018. Scaling accurate genetic variant discovery to tens of thousands of samples. bioRxiv:201178.

Ptak SE, Hinds DA, Koehler K, Nickel B, Patil N, Ballinger DG, Przeworski M, Frazer KA, Paabo S. 2005. Fine-scale recombination patterns differ between chimpanzees and humans. Nat Genet 37:429-434.

Quinlan AR, Hall IM. 2010. BEDTools: a flexible suite of utilities for comparing genomic features. Bioinformatics 26:841-842.

R Core Team. 2021. R: A language and environment for statistical computing. Vienna, Austria.

Ranwez V, Douzery EJP, Cambon C, Chantret N, Delsuc F. 2018. MACSE v2: Toolkit for the Alignment of Coding Sequences Accounting for Frameshifts and Stop Codons. Mol Biol Evol 35:2582-2584.

Revell LJ. 2012. phytools: an R package for phylogenetic comparative biology (and other things). Methods in Ecology and Evolution 3:217-223.

Rivas-Gonzalez I, Rousselle M, Li F, Zhou L, Dutheil JY, Munch K, Shao Y, Wu D, Schierup MH, Zhang G. 2023. Pervasive incomplete lineage sorting illuminates speciation and selection in primates. Science 380:eabn4409.

Robinson DF, Foulds LR. 1981. Comparison of phylogenetic trees. Mathematical Biosciences 53:131-147.

Robinson DF, Foulds LR editors.; 1979 Berlin, Heidelberg.

Romanenko SA, Perelman PL, Trifonov VA, Graphodatsky AS. 2012. Chromosomal evolution in Rodentia. Heredity (Edinb) 108:4-16.

Rosenberg NA. 2002. The probability of topological concordance of gene trees and species trees. Theor Popul Biol 61:225-247.

Rowe KC, Achmadi AS, Fabre P-H, Schenk JJ, Steppan SJ, Esselstyn JA. 2019. Oceanic islands of Wallacea as a source for dispersal and diversification of murine rodents. Journal of Biogeography 46:2752-2768.

Roycroft E, Achmadi A, Callahan CM, Esselstyn JA, Good JM, Moussalli A, Rowe KC. 2021. Molecular Evolution of Ecological Specialisation: Genomic Insights from the Diversification of Murine Rodents. Genome Biol Evol 13:evab103.

Roycroft EJ, Moussalli A, Rowe KC. 2020. Phylogenomics Uncovers Confidence and Conflict in the Rapid Radiation of Australo-Papuan Rodents. Syst Biol 69:431-444.

Sarver BA, Keeble S, Cosart T, Tucker PK, Dean MD, Good JM. 2017. Phylogenomic Insights into Mouse Evolution Using a Pseudoreference Approach. Genome Biol Evol 9:726-739.

Scally A, Dutheil JY, Hillier LW, Jordan GE, Goodhead I, Herrero J, Hobolth A, Lappalainen T, Mailund T, Marques-Bonet T, et al. 2012. Insights into hominid evolution from the gorilla genome sequence. Nature 483:169-175.

Schenk JJ, Rowe KC, Steppan SJ. 2013. Ecological opportunity and incumbency in the diversification of repeated continental colonizations by muroid rodents. Syst Biol 62:837-864.

1209

1210   Schliep KP. 2011. phangorn: phylogenetic analysis in R. Bioinformatics 27:592-593.

1211

1212   Serizawa K, Suzuki H, Tsuchiya K. 2000. A phylogenetic view on species radiation in Apodemus

1213   inferred from variation of nuclear and mitochondrial genes. Biochem Genet 38:27-40.

1214

1215   Shifman S, Bell JT, Copley RR, Taylor MS, Williams RW, Mott R, Flint J. 2006. A high-resolution

1216   single nucleotide polymorphism genetic map of the mouse genome. PLoS Biol 4:e395.

1217

1218   Singhal S, Leffler EM, Sannareddy K, Turner I, Venn O, Hooper DM, Strand AI, Li Q, Raney B,

1219   Balakrishnan CN, et al. 2015. Stable recombination hotspots in birds. Science 350:928-932.

1220

1221   Slatkin M, Pollack JL. 2006. The concordance of gene trees and species trees at two linked loci.

1222   Genetics 172:1979-1984.

1223

1224   Smagulova F, Gregoretti IV, Brick K, Khil P, Camerini-Otero RD, Petukhova GV. 2011. Genome-

1225   wide analysis reveals novel molecular features of mouse recombination hotspots. Nature 472:375-

1226   378.

1227

1228   RepeatMasker Open-4.0 [Internet]. 2013-2015. Available from http://www.repeatmasker.org.

1229

1230   Smith BT, Merwin J, Provost KL, Thom G, Brumfield RT, Ferreira M, Mauck WM, Moyle RG,

1231   Wright TF, Joseph L. 2023. Phylogenomic Analysis of the Parrots of the World Distinguishes

1232   Artifactual from Biological Sources of Gene Tree Discordance. Syst Biol 72:228-241.

1233

1234   Smith MD, Wertheim JO, Weaver S, Murrell B, Scheffler K, Kosakovsky Pond SL. 2015a. Less

1235   is more: an adaptive branch-site random effects model for efficient detection of episodic

1236   diversifying selection. Mol Biol Evol 32:1342-1353.

1237

1238   Smith SA, Brown JW, Walker JF. 2018. So many genes, so little time: A practical approach to

1239   divergence-time estimation in the genomic era. PLoS One 13:e0197433.

1240

1241   Smith SA, Moore MJ, Brown JW, Yang Y. 2015b. Analysis of phylogenomic datasets reveals

1242   conflict, concordance, and gene duplications with examples from animals and plants. BMC Evol

1243   Biol 15:150.

1244

1245   Stanyon R, Yang F, Cavagna P, O'Brien P, Bagga M, Ferguson-Smith M, Wienberg J. 1999.

1246   Animal Cytogenetics and Comparative Mapping-Reciprocal chromosome painting shows that

genomic rearrangement between rat and mouse proceeds ten times faster than between humans and cats. Cytogenetics and Cell Genetics 84:150-155.

Stapley J, Feulner PGD, Johnston SE, Santure AW, Smadja CM. 2017. Variation in recombination frequency and distribution across eukaryotes: patterns and processes. Philos Trans R Soc Lond B Biol Sci 372.

Steenwyk JL, Li Y, Zhou X, Shen XX, Rokas A. 2023. Incongruence in the phylogenomics era. Nat Rev Genet 24:834-850.

Steppan SJ, Adkins RM, Spinks PQ, Hale C. 2005. Multigene phylogeny of the Old World mice, Murinae, reveals distinct geographic lineages and the declining utility of mitochondrial genes compared to nuclear genes. Mol Phylogenet Evol 37:370-388.

Steppan SJ, Schenk JJ. 2017. Muroid rodent phylogenetics: 900-species tree reveals increasing diversification rates. PLoS One 12:e0183070.

Stevison LS, Woerner AE, Kidd JM, Kelley JL, Veeramah KR, McManus KF, Great Ape Genome P, Bustamante CD, Hammer MF, Wall JD. 2016. The Time Scale of Recombination Rate Evolution in Great Apes. Mol Biol Evol 33:928-945.

Sun C, Huang J, Wang Y, Zhao X, Su L, Thomas GWC, Zhao M, Zhang X, Jungreis I, Kellis M, et al. 2021. Genus-Wide Characterization of Bumblebee Genomes Provides Insights into Their Evolution and Variation in Ecological and Behavioral Traits. Mol Biol Evol 38:486-501.

Suzuki H, Shimada T, Terashima M, Tsuchiya K, Aplin K. 2004. Temporal, spatial, and ecological modes of evolution of Eurasian Mus based on mitochondrial and nuclear gene sequences. Mol Phylogenet Evol 33:626-646.

Tange O. 2018. GNU Parallel.

To TH, Jung M, Lycett S, Gascuel O. 2016. Fast Dating Using Least-Squares Criteria and Algorithms. Syst Biol 65:82-97.

Treaster S, Deelen J, Daane JM, Murabito J, Karasik D, Harris MP. 2023. Convergent genomics of longevity in rockfishes highlights the genetics of human life span variation. Sci Adv 9:eadd2743.

1285 van der Valk T, Pecnerova P, Diez-Del-Molino D, Bergstrom A, Oppenheimer J, Hartmann S,
1286 Xenikoudakis G, Thomas JA, Dehasque M, Saglican E, et al. 2021. Million-year-old DNA sheds
1287 light on the genomic history of mammoths. Nature 591:265-269.

1288

1289 Vanderpool D, Minh BQ, Lanfear R, Hughes D, Murali S, Harris RA, Raveendran M, Muzny DM,
1290 Hibbins MS, Williamson RJ, et al. 2020. Primate phylogenomics uncovers multiple rapid
1291 radiations and ancient interspecific introgression. PLoS Biol 18:e3000954.

1292

1293 Wang LG, Lam TT, Xu S, Dai Z, Zhou L, Feng T, Guo P, Dunn CW, Jones BR, Bradley T, et al.
1294 2020. Treeio: An R Package for Phylogenetic Tree Input and Output with Richly Annotated and
1295 Associated Data. Mol Biol Evol 37:599-603.

1296

1297 White MA, Ane C, Dewey CN, Larget BR, Payseur BA. 2009. Fine-scale phylogenetic
1298 discordance across the house mouse genome. PLoS Genet 5:e1000729.

1299

1300 Yalcin B, Wong K, Agam A, Goodson M, Keane TM, Gan X, Nellaker C, Goodstadt L, Nicod J,
1301 Bhomra A, et al. 2011. Sequence-based characterization of structural variation in the mouse
1302 genome. Nature 477:326-329.

1303

1304 Yang Z. 2007. PAML 4: phylogenetic analysis by maximum likelihood. Mol Biol Evol 24:1586-
1305 1591.

1306

1307 Yekutieli D, Benjamini Y. 1999. Resampling-based false discovery rate controlling multiple test
1308 procedures for correlated test statistics. Journal of Statistical Planning and Inference 82:171-196.

1309

1310 Yu G. 2020. Using ggtree to Visualize Data on Tree-Like Structures. Curr Protoc Bioinformatics
1311 69:e96.

1312

1313 Yu G, Smith DK, Zhu H, Guan Y, Lam TT-Y. 2017. ggtree: an r package for visualization and
1314 annotation of phylogenetic trees with their covariates and other associated data. Methods in
1315 Ecology and Evolution 8:28-36.

1316

1317 Zhang C, Rabiee M, Sayyari E, Mirarab S. 2018. ASTRAL-III: polynomial time species tree
1318 reconstruction from partially resolved gene trees. BMC Bioinformatics 19:153.

1319

1320

1321